

Cluster Regularization via a Hierarchical Feature Regression

Johann Pfitzinger^a

^a*Goethe University, Frankfurt am Main*

Abstract

Prediction tasks with high-dimensional nonorthogonal predictor sets pose a challenge for least squares based fitting procedures. A large and productive literature exists, discussing various regularized approaches to improving the out-of-sample robustness of parameter estimates. This paper proposes a novel cluster-based regularization — the hierarchical feature regression (HFR) —, which mobilizes insights from the domains of machine learning and graph theory to estimate parameters along a supervised hierarchical representation of the predictor set, shrinking parameters towards group targets. The method is innovative in its ability to estimate optimal compositions of predictor groups, as well as the group targets endogenously. The HFR can be viewed as a supervised factor regression, with the strength of shrinkage governed by a penalty on the extent of idiosyncratic variation captured in the fitting process. The method demonstrates good predictive accuracy and versatility, outperforming a panel of benchmark regularized estimators across a diverse set of simulated regression tasks, including dense, sparse and grouped data generating processes. An application to the prediction of economic growth is used to illustrate the HFR’s effectiveness in an empirical setting, with favorable comparisons to several frequentist and Bayesian alternatives.

Keywords: Regularization, group shrinkage, graph theory, machine learning, hierarchical clustering

JEL classification C13, C53, C55, O47

Email address: johann.pfitzinger@gmail.com (Johann Pfitzinger)

This paper represents a chapter of my PhD thesis submitted at Goethe University Frankfurt. I thank my supervisor Uwe Hassler for his advice.

1. Introduction

In this paper, I present a new solution to the old problem of calculating robust parameter estimates in a regression with nonorthogonal predictors. A standard linear least squares regression is regularized by shrinking estimates towards group target values using a hierarchical transformation of the parameter space. The resulting estimator has a number of useful properties: (i) It solves the problem of group mean shrinkage in an elegant and efficient manner, where the composition of parameter groups as well as group shrinkage targets are determined endogenously, using a single intuitive hyperparameter; (ii) While it is conceptually related to latent variable regressions, with a penalty on the complexity of signal variation, the construction of factor spaces is entirely supervised; (iii) The estimator exhibits significant versatility, performing well (in terms of prediction accuracy) both in sparse, as well as dense regression settings; Finally, (iv) the estimator encodes the prior expectation of a world governed by hierarchical processes, making it uniquely suitable for several empirical applications, particularly in the domains of economics and finance.

A substantial literature exists on regularized regression techniques, the main thrust of which comprises variants of penalized or latent variable regressions, and which finds its most general expression in the extensive field of Bayesian regression analysis. With increasing availability of data, regularized regressions have steadily grown in importance in many fields, and underpin important developments in domains as seemingly disparate as bioinformatics, finance or deep learning. Economic applications in particular are often characterized by high-dimensional, multicollinear data sets, and regularized machine learning algorithms are well established as computationally efficient means of obtaining stable and accurate parameter estimates when the number of predictors relative to observations is high. The hierarchical feature regression (HFR) proposed here contributes to this body of knowledge, combining elements of graph theory and machine learning to inform a novel group shrinkage estimator.

The HFR constructs a parsimonious information hierarchy, clustering predictors based on the similarity of their explanatory content with respect to a dependent variable. The information hierarchy is translated into a parameter hierarchy, consisting of several chains of coefficients that capture increasingly nuanced signal. The coefficient chains adjust first for shared variation, with each lower element introducing a further degree of idiosyncrasy. By shrinking the chain of coefficients, the HFR achieves group mean shrinkage — removing idiosyncratic information from the fitting process and giving a higher weight to shared signal patterns. Rather than allowing each predictor to enter the fitting process as a direct substitute to all other predictors, related predictors compete

only for variance not explained by their common patterns. Thus, instead of simply reducing the size of parameter estimates, the HFR exploits information about the relatedness of predictors to shrink parameter estimates towards group target values.

In doing so, the HFR departs from the mainstream of the regularization literature (e.g. it does not perform variable selection). Nonetheless, the method demonstrates considerable versatility in a simulated setting, outperforming a panel of benchmark regularized regression techniques across a diverse set of regression tasks that include grouped, sparse and latent factor designs. In all of the simulations, the HFR presents superior or closely matched predictive accuracy when compared to commonly used penalized, as well as latent variable regressions. The key advantage is its flexibility. Where related methods tend to be best suited to specialized types of tasks, the HFR is found to produce accurate parameter estimates across a spectrum of data generating processes.

An empirical application using a widely applied data set of economic growth determinants showcases the estimator’s performance in a real-world setting with many correlated predictors and a (presumably) sparse data generating process. The HFR achieves the lowest out-of-sample prediction errors, comparing favorably to benchmark frequentist and Bayesian methods. Apart from generating accurate predictions, the hierarchical structure of the HFR can be used to extract insights about the underlying latent dynamics of economic growth disparities, with few factors — primarily regional and geographic in nature — explaining a substantial portion of the observed variation.

The remainder of this paper is structured as follows: Section 2 introduces important literature relating to the field of regularized regression. The HFR is developed in Section 3, while Sections 4 and 5 explore its performance in a simulated and empirical setting. Section 6 discusses extensions and potential future work, and, finally, Section 7 concludes the paper.

2. Literature review

Nobel prize laureate Herbert Simon posits that complex systems tend to evolve in a hierachic manner and, as a result, encompass hierarchical structures (Simon, 1962). This proposition is supported by an understanding of highly integrated markets and economies driven in part by deeper global undercurrents (e.g. global business cycles (Diebold & Yilmaz, 2015; Kose *et al.*, 2003) or global financial cycles (Rey, 2015)) and is reflected in the popularity of latent variable methods (e.g. dynamic factor models for macroeconometric analysis) and, increasingly, deep learning meth-

ods for nonlinear prediction tasks.³

The HFR utilizes empirical data hierarchies with the objective of achieving an optimal group mean shrinkage that captures the hierarchical nature of the data generating processes, and, in turn, attains more robust out-of-sample performance. It is therefore located squarely within the regularization literature. A plethora of approaches to parameter regularization have been developed in this domain. Penalized regressions — termed “Lasso and friends” in [Varian \(2014\)](#) — receive some attention in this paper as natural benchmarks for the HFR. The approaches introduce a constraint on the parameter norm, by adding a penalty function $P_\lambda(\beta)$ to the least squares loss of a regression of y on \mathbf{x} :

$$\hat{\beta} = \arg \min_{\beta} \left[N^{-1} (y - \mathbf{x}\beta)' (y - \mathbf{x}\beta) + P_\lambda(\beta) \right]. \quad (2.1)$$

Here $\hat{\beta}$ is a vector of parameter estimates and N is the sample size. The penalty function depends on a hyperparameter λ governing the weight given to the penalty, and typically takes the form $P_\lambda(\beta) = \lambda \sum_i |\beta_i|^q$, where $q = 1$ is a Lasso and $q = 2$ is a ridge regression. Important contributions to this literature include [James & Stein \(1961\)](#), [Hoerl \(1962\)](#), [Hoerl & Kennard \(1970\)](#), [Tibshirani \(1996\)](#) and [Efron *et al.* \(2004\)](#), as well as multiple variants, including [Zou & Hastie \(2005\)](#), [Zou \(2006\)](#) and [Zou & Zhang \(2009\)](#). An introductory overview is found in [Friedman *et al.* \(2001\)](#).

Penalized regressions — particularly those based on the ℓ_1 -norm ($q = 1$) — have been extended to permit group shrinkage ([Bondell & Reich, 2008](#); [Tibshirani *et al.*, 2005](#); [Turlach *et al.*, 2005](#); [Yuan & Lin, 2006](#); [Zeng & Figueiredo, 2013](#)). A good review of available approaches is given in [Bach *et al.* \(2012\)](#). Group shrinkage typically aims to shrink disjoint or overlapping groups of variables towards zero, often requiring prior knowledge of groups. The HFR differs from these methods in that sparsity is not an objective and group compositions are estimated endogenously without the need for external structures.

Conceptually, the type of group mean shrinkage performed by the HFR can be achieved in a penalized regression framework, for instance, by generalizing the ridge regression to the following form ([Hansen, 2019](#); [van Wieringen, 2020](#)):

³Deep neural networks, for instance, can be viewed as nonlinear hierarchical feature machines ([Mishra & Gupta, 2017](#)).

$$\hat{\beta} = \arg \min_{\beta} [(y - \mathbf{x}\beta)'(y - \mathbf{x}\beta) + (\beta_0 - \beta)' \Delta (\beta_0 - \beta)], \quad (2.2)$$

where Δ governs the speed and direction of shrinkage for each parameter individually, and β_0 contains a shrinkage target for each parameter. The target values can be set in such a way as to induce group mean shrinkage, by selecting the same shrinkage target for groups of variables, and specifying penalties in Δ on a group-specific basis. This requires *a priori* definitions of group compositions and target values, reducing its practicality.

A second broad class of regularization techniques are latent variable regressions. Examples include the principal components regression (PCR) described in [Friedman *et al.* \(2001\)](#), the partial least squares regression (PLSR) developed by Wold in the 1960s and 70s (see [Wold \(2001\)](#) and [Martens \(2001\)](#)), or — in the econometric setting — the dynamic factor model surveyed in [Stock & Watson \(2016a\)](#) and [Stock & Watson \(2016b\)](#). These methods reduce the dimensionality of the predictor set by removing low variance components in the case of principal components based methods, or components with a low response correlation in the case of PLSR ([Jolliffe, 2002](#)). [Jolliffe \(2002\)](#) and [van Wieringen \(2020\)](#) show that the PCR is closely related to biased estimation techniques such as the ridge regression, however unlike penalized regressions, latent variable regressions are mostly unsupervised in their construction of common factors. Some exceptions exist, for instance the aforementioned PLSR, or [Bair *et al.* \(2006\)](#), who introduce a (semi-)supervised PCR, by using a supervised process of pre-filtering the predictor set before performing principal components analysis.

The HFR constructs factors using a hierarchical transformation of the predictors. The concept of feature hierarchies has been applied in the machine learning domain to visual and text classification tasks, where general features (e.g. objects, phrases) are learned first, with subsequent fine-tuning for lower level representations (e.g. pixels, words) ([Epshtain & Uliman, 2005](#); [Girshick *et al.*, 2014](#)). The HFR ports this concept to the linear regression setting, where the feature hierarchy can be exploited to increase the robustness of parameter estimates in a manner not unrelated to its role in learning invariant representations in text and image data. The HFR decomposes the data generating process (DGP) into a hierarchical signal structure, estimating parameters for general (shared) signal patterns separately from the idiosyncratic contribution of each individual predictor.

Hierarchical clustering algorithms (a sub-field of unsupervised machine learning) present an approach to explicitly estimating the type of data hierarchies used by the HFR, and have been

applied in multiple domains, including financial time series (Di Matteo *et al.*, 2004; León *et al.*, 2017; Mantegna, 1999; Tola *et al.*, 2008; Tumminello *et al.*, 2010). Recent applications in the portfolio construction literature have resulted in an interesting conceptual pendant to the HFR (Alipour *et al.*, 2016; Lopez de Prado, 2016; Pfitzinger & Katzke, 2019; Raffinot, 2016). The authors find that portfolios of financial assets can be enhanced by replacing pairwise correlations with group-wise correlations of asset return series. This reasoning is not unlike the mechanism by which the HFR achieves more robust parameter estimates.

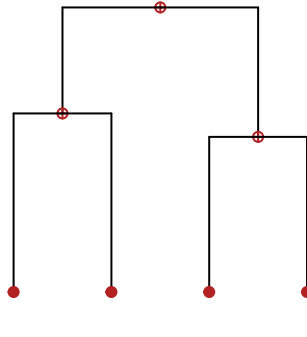
3. The HFR estimator

3.1. *Syntax of feature hierarchies*

Before introducing the HFR estimator, this section provides a brief overview of the graph theoretical concepts and definitions drawn on in the subsequent discussions.

A hierarchical representation is taken to mean the arrangement of predictors into clusters of two or more, which are merged at nodes to form higher levels. The predictors are the leaf nodes (i.e. they represent the lowest nodes in the hierarchy), while nodes at higher levels are called internal nodes. The process of merging is repeated at each level until all predictors are contained within a single cluster called the root node. The node directly above any node is typically referred to as the parent node, while the nodes below are the children. Adjacent nodes that share a single parent are siblings. The chain of preceding parent nodes for any node is its branch.

Hierarchies can be depicted graphically in dendrograms, or mathematically in summing matrices. Figure 3.1 portrays a simple hierarchy dendrogram of the illustration introduced in Section 3.2. There are $K = 4$ predictors (leaf nodes), and two subsets grouping two predictors each. The root node completes the hierarchy dendrogram.



$$S = \begin{bmatrix} 1 & 1 & 1 & 1 \\ 1 & 1 & 0 & 0 \\ 0 & 0 & 1 & 1 \\ 1 & 0 & 0 & 0 \\ 0 & 1 & 0 & 0 \\ 0 & 0 & 1 & 0 \\ 0 & 0 & 0 & 1 \end{bmatrix}$$

Figure 3.1: Example of a hierarchy dendrogram (left) and the corresponding summing matrix (right).

The corresponding hierarchy summing matrix S (right panel, Fig. 3.1) consists of $D \times K$ dimensions, where $D = 7$ is the total number of nodes and $K = 4$ is the number of predictors. S is invariant to the ordering of rows (i.e. child and parent nodes do not have to be arranged in any particular order). However, to simplify the discussion it is presented in a top-down order throughout this paper, starting with the root node and ending with the leaf nodes.

Hierarchies can be cut along the y -axis of the dendrogram by drawing a horizontal line at any height of Fig. 3.1. The nodes directly beneath the cut describe a level. In the discussions that follow an arbitrary level is denoted ℓ , and L is the total number of levels. Fig. 3.2 shows a cut in the dendrogram and the summing matrix associated with that level:

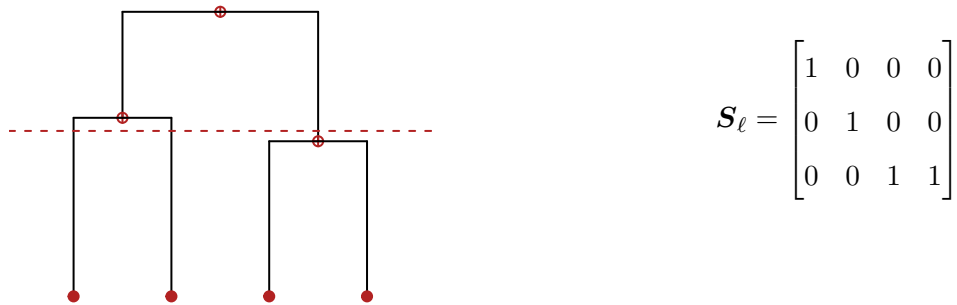


Figure 3.2: Example of a cut hierarchy dendrogram (left) and the corresponding level-specific summing matrix (right).

A predictor hierarchy conveys information about the interrelatedness of predictors, grouping similar predictors closely together based on some dissimilarity metric. In the context of the HFR, coefficients on predictors whose paths merge within the hierarchy experience shrinkage towards

a common target. The higher in the hierarchy the merge is located, the stronger the shrinkage. In Sections 3.2 to 3.4, the HFR is introduced under the assumption of a given optimal hierarchy, while Section 3.5 introduces an algorithm to estimate \mathbf{S} .

3.2. A framework for group mean shrinkage

The hierarchical feature regression is introduced in this section using a simple example, and following two steps: First, a decomposition of the ordinary least squares (OLS) estimator into a sequence of level-specific components is proposed. Second, shrinkage is introduced to the level-specific components resulting in the HFR estimator. The simple example is eventually generalized in the subsequent sections.

To introduce the decomposition of the OLS estimator into hierarchical components, take again the setting described above with $K = 4$ standardized predictors, $\mathbf{x} = \{\mathbf{x}_i\}_{i=1,\dots,N} \in \mathbb{R}_K$, which are clustered into one, two and four groups, resulting in the summing matrix given in Fig. 3.1 and below. The matrix \mathbf{S} is assumed to represent an optimal clustering, with similar variables situated adjacently:

$$\mathbf{S} = \begin{bmatrix} 1 & 1 & 1 & 1 \\ 1 & 1 & 0 & 0 \\ 0 & 0 & 1 & 1 \\ 1 & 0 & 0 & 0 \\ 0 & 1 & 0 & 0 \\ 0 & 0 & 1 & 0 \\ 0 & 0 & 0 & 1 \end{bmatrix}.$$

The summing matrix can be divided into sub-matrices, denoted \mathbf{S}_ℓ , which describe the individual levels within the simple feature hierarchy, such that with $\ell = 1, 2, 3$

$$\mathbf{S}_1 = \begin{bmatrix} 1 & 1 & 1 & 1 \end{bmatrix} \quad \mathbf{S}_2 = \begin{bmatrix} 1 & 1 & 0 & 0 \\ 0 & 0 & 1 & 1 \end{bmatrix} \quad \mathbf{S}_3 = \begin{bmatrix} 1 & 0 & 0 & 0 \\ 0 & 1 & 0 & 0 \\ 0 & 0 & 1 & 0 \\ 0 & 0 & 0 & 1 \end{bmatrix}.$$

Here the lowest level (\mathbf{S}_3) is an identity matrix containing the leaf nodes.

Now, define $\mathbf{z}_\ell = \mathbf{x}\mathbf{S}'_\ell$ as the level-specific hierarchical features. The complete hierarchical feature set is given by $\mathbf{z} = \mathbf{x}\mathbf{S}' = [\mathbf{z}_1 \ \mathbf{z}_2 \ \mathbf{z}_3]$. The hierarchical features, \mathbf{z} , represent factor estimates of the common variance contained in the child features (i.e. the features associated with child nodes). Under the assumption that the covariance between the idiosyncratic components of the child features is low (with the mean of idiosyncratic components converging to zero), the sum of the covariates represents an estimate of the common component that is consistent up to a constant scale. See [Stock & Watson \(2016b\)](#) for a discussion of the role of feature averaging in factor estimation.

Using the level-specific factor estimates, define $\mathbf{Q}_{ij} = \mathbf{z}'_i \mathbf{z}_j$, $i, j \in \{1, 2, 3\}$, and $\mathbf{Q}_{\ell y} = \mathbf{z}'_\ell \mathbf{M}_{\ell-1} y$, with the regression response variable $y = \{y_i\}_{i=1,\dots,N} \in \mathbb{R}$. Furthermore, \mathbf{M}_ℓ is the residual maker matrix, with $\mathbf{M}_\ell = \mathbf{I}_N - \mathbf{P}_\ell = \mathbf{I}_N - \mathbf{z}_\ell \mathbf{Q}_{\ell\ell}^{-1} \mathbf{z}'_\ell$, and $\mathbf{M}_0 = \mathbf{I}_N$. Here \mathbf{I}_N is an $N \times N$ dimensional identity matrix. The role of $\mathbf{M}_{\ell-1}$ is to partial out the effect of each node's branch from $\mathbf{Q}_{\ell y}$, resulting in a regression that updates parameter estimates using only the new information introduced at each level in a top-down manner.

With $\hat{\beta}_{\text{ols}}$ denoting ordinary least squares (OLS) estimates for a regression of y on \mathbf{x} , a top-down hierarchical decomposition of the OLS estimator is given by

$$\hat{\beta}_{\text{ols}} = \hat{\mathbf{b}}_1 + \hat{\mathbf{b}}_2 + \hat{\mathbf{b}}_3, \quad (3.1)$$

where $\hat{\mathbf{b}}_\ell = \mathbf{S}'_\ell \hat{\beta}_\ell$, and $\hat{\beta}_\ell$ are level-specific estimates that account for the new idiosyncratic variation introduced at level ℓ . The level-specific estimates are defined simply as the least squares estimates for \mathbf{z}_ℓ conditional on the path of each node:

$$\hat{\beta}_\ell = \mathbf{Q}_{\ell\ell}^{-1} \mathbf{Q}_{\ell y}. \quad (3.2)$$

The hierarchical decomposition therefore consists of an additive chain of level-specific estimates that iteratively adjust for idiosyncratic variation in the fitting process in a top-down manner, until at the final level ($\ell = 3$ in the example) all explainable variation is accounted for. While this decomposition seems trivial at first glance, it can be used as the basis for a regularized regression. The HFR estimator shrinks the extent to which levels are permitted to adjust for idiosyncratic

variation, resulting in estimates that are biased towards higher-level representations in the form of group means for clusters of covariates. Proposition 1 stacks the above decomposition into a single equation, while the proof in [Appendix A](#) shows that the resulting estimates are numerically equivalent to OLS estimates:

Proposition 1. *Consider a simple regression decomposition for the case of $L = 3$ with a given summing matrix \mathbf{S} , hierarchical features \mathbf{z} defined as above, and $\mathbf{Q}_{ij} = \mathbf{z}'_i \mathbf{z}_j$,*

$$\mathbf{Q}_{zz} = \begin{bmatrix} \mathbf{Q}_{11} & \mathbf{0} & \mathbf{0} \\ \mathbf{Q}_{21} & \mathbf{Q}_{22} & \mathbf{0} \\ \mathbf{Q}_{31} & \mathbf{Q}_{32} & \mathbf{Q}_{33} \end{bmatrix} \quad \text{and} \quad \mathbf{Q}_{zy} = \mathbf{z}' y.$$

Now the coefficient estimates $\hat{\beta} = \mathbf{S}' \mathbf{Q}_{zz}^{-1} \mathbf{Q}_{zy}$ represent least squares optimal estimates of the linear slope coefficients β of a regression of y on \mathbf{x} .

The proof of Proposition 1 is given in [Appendix A](#). Note that \mathbf{Q}_{zz} can be written as $\mathbf{Q}_{zz} = \mathbf{z}' \mathbf{z} \odot \mathbf{H}$, where \odot is the element-wise multiplication operator, and \mathbf{H} is a matrix of ones with the block-wise upper triangle set to zero:

$$\mathbf{H} = \begin{bmatrix} \mathbf{1} & \mathbf{0} & \mathbf{0} \\ \mathbf{1} & \mathbf{1} & \mathbf{0} \\ \mathbf{1} & \mathbf{1} & \mathbf{1} \end{bmatrix}, \quad \mathbf{1} = \begin{bmatrix} 1 & \cdots & 1 \\ \vdots & \ddots & \vdots \\ 1 & \cdots & 1 \end{bmatrix}, \quad \mathbf{0} = \begin{bmatrix} 0 & \cdots & 0 \\ \vdots & \ddots & \vdots \\ 0 & \cdots & 0 \end{bmatrix}.$$

As shown in [Appendix A](#), Proposition 1 is equivalent to the chain of level-specific estimates introduced in Eq. 3.1, with

$$\hat{\beta} = \mathbf{S}' \mathbf{Q}_{zz}^{-1} \mathbf{Q}_{zy} \tag{3.3}$$

$$= \mathbf{S}' \text{vec}(\hat{\beta}_1, \hat{\beta}_2, \hat{\beta}_3) \tag{3.4}$$

$$= \hat{\mathbf{b}}_1 + \hat{\mathbf{b}}_2 + \hat{\mathbf{b}}_3. \tag{3.5}$$

When shrinkage is introduced to Eq. 3.3, the resulting estimates are biased towards group means,

since lower levels are not permitted to adjust fully to the idiosyncratic information contained in them. In the simplest form, one could add a shrinkage coefficient to Eq. 3.1, such that

$$\hat{\beta}^* = \sum_{\ell=1}^3 \theta_\ell \hat{b}_\ell, \quad (3.6)$$

where θ_ℓ is the ℓ th shrinkage coefficient, with $0 \leq \theta_\ell \leq 1$. For instance, if $\theta_2 = \theta_3 = 0$ and $\theta_1 = 1$, the estimates are reduced to $\hat{\beta}^* = \hat{b}_1$, which is equivalent to a single group mean across all parameters. In the stacked form used in Proposition 1, shrinkage could be applied directly to \mathbf{Q}_{zz} in a manner analogous to a generalized ridge regression projected to the hierarchical feature dimension, by adding a block diagonal to the matrix:

$$\hat{\beta}^* = \mathbf{S}'(\mathbf{Q}_{zz} + \boldsymbol{\Theta})^{-1}\mathbf{Q}_{zy} = \mathbf{S}' \left(\begin{bmatrix} \mathbf{Q}_{11} & \mathbf{0} & \mathbf{0} \\ \mathbf{Q}_{21} & \mathbf{Q}_{22} & \mathbf{0} \\ \mathbf{Q}_{31} & \mathbf{Q}_{32} & \mathbf{Q}_{33} \end{bmatrix} + \begin{bmatrix} \boldsymbol{\Theta}_1 & \mathbf{0} & \mathbf{0} \\ \mathbf{0} & \boldsymbol{\Theta}_2 & \mathbf{0} \\ \mathbf{0} & \mathbf{0} & \boldsymbol{\Theta}_3 \end{bmatrix} \right)^{-1} \mathbf{Q}_{zy}. \quad (3.7)$$

Here $\boldsymbol{\Theta}_\ell$ governs the extent of shrinkage for level ℓ . Eq. 3.7 is equivalent to a generalized ridge regression translated to the hierarchical feature space. It is generalized in the sense that individual levels experience shrinkage at differing paces, captured in the level-wise penalties $\boldsymbol{\Theta}_\ell$. As will be shown in Section 3.4, formulating shrinkage in a multiplicative, as opposed to additive, manner vastly simplifies the optimization. Thus, Eq. 3.7 is replaced by Eq. 3.8 (where each $\boldsymbol{\Theta}_\ell$ has D rows, and $\boldsymbol{\Theta}$ is no longer block-diagonal):

$$\hat{\beta}_{\text{hfr}} = \mathbf{S}'(\mathbf{Q}_{zz} \odot \boldsymbol{\Theta})^{-1}\mathbf{Q}_{zy} = \mathbf{S}' \left(\begin{bmatrix} \mathbf{Q}_{11} & \mathbf{0} & \mathbf{0} \\ \mathbf{Q}_{21} & \mathbf{Q}_{22} & \mathbf{0} \\ \mathbf{Q}_{31} & \mathbf{Q}_{32} & \mathbf{Q}_{33} \end{bmatrix} \odot \begin{bmatrix} \boldsymbol{\Theta}_1 & \boldsymbol{\Theta}_2 & \boldsymbol{\Theta}_3 \end{bmatrix} \right)^{-1} \mathbf{Q}_{zy}. \quad (3.8)$$

Eq. 3.8 is the HFR estimator under the assumption that the hierarchy (\mathbf{S}) as well as the extent of shrinkage ($\boldsymbol{\Theta}$) are given. Multiplying \mathbf{Q}_{zz} with the shrinkage matrix (as opposed to adding a block-diagonal matrix) induces shrinkage at a linear rate, with all node-specific parameter estimates in a single level shrunken towards zero at a rate directly proportional to the size of the penalty for that level. The equation represents a stacked version of Eq. 3.6, with shrinkage coefficients applied to each level-specific parameter vector, and

$$\Theta_\ell = \begin{bmatrix} \theta_\ell^{-1} & \cdots & \theta_\ell^{-1} \\ \vdots & \ddots & \vdots \\ \theta_\ell^{-1} & \cdots & \theta_\ell^{-1} \end{bmatrix}.$$

Since the approach has the ability to remove entire levels from the regression (by setting $\theta_\ell = 0$), it can be used as a tool to select a parsimonious hierarchy based on a (potentially large) set of input levels. As shown in subsequent sections, this property will be useful for the estimation of \mathbf{S} .

The framework described by Eq. 3.8 can become arbitrarily complex, including a large number of levels that permit a high degree of nuance with respect to the nature and strength of regularization. The proposed framework decomposes each parameter into a sequence of parameters, which capture successively more idiosyncratic signal. This parameter chain is subsequently regularized, resulting in overall shrinkage towards a more general and less idiosyncratic representation of the data generating process. A key ingredient for this form of group mean shrinkage is determining the optimal extent of shrinkage for each hierarchical level (i.e. for the different elements of the parameter chain). Section 3.3 discusses an appropriate loss function that can be used to obtain optimal shrinkage coefficients.

3.3. Optimal shrinkage in the hierarchical feature regression

Generalizing the definition in Eq. 3.8, the hierarchical feature regression estimates, $\hat{\beta}_{\text{hfr}}$, are given by

$$\hat{\beta}_{\text{hfr}} = \mathbf{S}'(\mathbf{z}'\mathbf{z} \odot \mathbf{H} \odot \Theta)^{-1}\mathbf{z}'\mathbf{y}, \quad (3.9)$$

where \mathbf{H} , as before, is a matrix of ones and zeros, which ensures that the block-wise upper triangle of $\mathbf{z}'\mathbf{z}$ is zero. Θ is a $D \times D$ matrix controlling the extent of shrinkage on a level-by-level basis. Letting Θ_ℓ contain that subset of columns of Θ associated with nodes in level ℓ , Θ is defined as

$$\Theta = \begin{bmatrix} \Theta_1 & \cdots & \Theta_L \end{bmatrix} \quad \text{where} \quad \Theta_\ell = \begin{bmatrix} \theta_\ell^{-1} & \cdots & \theta_\ell^{-1} \\ \vdots & \ddots & \vdots \\ \theta_\ell^{-1} & \cdots & \theta_\ell^{-1} \end{bmatrix} \quad \forall \ell \in 1, \dots, L.$$

The extent of shrinkage is therefore governed entirely by the $L \times 1$ vector of level-specific shrinkage weights $\boldsymbol{\theta} = (\theta_1 \ \dots \ \theta_L)$. When $\boldsymbol{\theta} = \mathbf{1}$ there is no shrinkage, leading to the least squares optimal solution as shown in Proposition 1. If any $\theta_\ell < 1$, the parameters associated with level ℓ are regularized, where $\theta_\ell = 0$ constitutes maximum shrinkage. Finally, when $\theta_1 < 1$, all parameters are shrunken towards zero in a manner analogous to a ridge regression.

The objective of the HFR is to determine the optimal degree of shrinkage for each level ℓ , given some predefined hyperparameter, denoted λ , which captures — in a single number — the total extent of regularization to apply to the problem. As discussed, the least squares optimal solution is achieved when $\boldsymbol{\theta} = \mathbf{1}$. In order to obtain any degree of shrinkage, a penalty needs to be introduced to the loss function that induces $\theta_\ell < 1$. From an information theoretical vantage, a natural choice for the penalty is the effective degrees of freedom of $\hat{\boldsymbol{\beta}}_{\text{hfr}}$. This approach selects shrinkage weights by trading off overall model fit against parsimony. The number of nodes in the final level (i.e. the leaf nodes) is exactly equal to the number of covariates. Each preceding level has a strictly smaller number of nodes. As lower levels are regularized, the effective degrees of freedom (ν_{eff}), which is a positive function of the number of nodes contained in each level, decreases. The effective degrees of freedom of the HFR can be calculated using the projection matrix:

$$\nu_{\text{eff}} = \text{tr}(\mathbf{P}_{\text{hfr}}), \quad \mathbf{P}_{\text{hfr}} = \mathbf{z}(\mathbf{z}'\mathbf{z} \odot \mathbf{H} \odot \boldsymbol{\Theta})^{-1}\mathbf{z}'. \quad (3.10)$$

Now the optimal extent of shrinkage $\boldsymbol{\theta}_\lambda^*$, conditional on hyperparameter λ , is given by

$$\boldsymbol{\theta}_\lambda^* = \arg \min_{\boldsymbol{\theta}} \left[N^{-1}(\mathbf{x}\hat{\boldsymbol{\beta}}_{\text{hfr}} - \mathbf{y})'(\mathbf{x}\hat{\boldsymbol{\beta}}_{\text{hfr}} - \mathbf{y}) + \lambda \nu_{\text{eff}} \right] \quad \text{s.t.} \quad \mathbf{0} \leq \boldsymbol{\theta} \leq \mathbf{1}. \quad (3.11)$$

Note that Eq. 3.11 closely resembles an information criterion such as the AIC or BIC. Level-wise shrinkage parameters are thus chosen by trading off goodness-of-fit against simplicity, where the hyperparameter λ tilts the global trade-off towards goodness-of-fit as $\lambda \rightarrow 0$, or simplicity as $\lambda \rightarrow \infty$. The following section demonstrates that obtaining the optimal shrinkage vector $\boldsymbol{\theta}_\lambda^*$ for any given level of λ is equivalent to solving a quadratic program, resulting in an efficient solution algorithm for Eq. 3.11.

3.4. Formulating the HFR as a quadratic program

The HFR estimates in Eq. 3.9 can be restated as the dot product of level-specific estimates and a transformed shrinkage vector, such that

$$\hat{\beta}_{\text{hfr}} = \hat{\mathbf{B}}\phi. \quad (3.12)$$

Here $\hat{\mathbf{B}}$ stacks unconditional level-specific estimates (unconditional with respect to preceding levels in the hierarchy), such that with $\hat{\mathbf{B}} = [\hat{\mathbf{w}}_1 \dots \hat{\mathbf{w}}_L]$, $\hat{\mathbf{w}}_\ell = \mathbf{S}'_\ell (\mathbf{z}'_\ell \mathbf{z}_\ell)^{-1} \mathbf{z}'_\ell \mathbf{y}$. Note that $\hat{\mathbf{w}}_\ell$ is an unconditional counterpart to $\hat{\mathbf{b}}_\ell$, where the effect of each node's branch has not been partialled out. Furthermore, ϕ is a transformation of θ that satisfies the equality $\theta = \phi' \omega$, where ω is a lower triangular matrix, resulting in

$$\phi = \begin{cases} \theta_\ell - \theta_{\ell+1} & \text{when } \ell < L \\ \theta_\ell & \text{otherwise.} \end{cases}$$

The derivation of Eq. 3.12 is given in [Appendix B](#), and follows directly from the introduction of shrinkage weights to the calculations in [Appendix A](#). By reformulating the problem in an unconditional manner, $\hat{\mathbf{w}}_\ell$ can be computed in parallel for each level, and the optimization of θ can be split into two consecutive steps: (i) estimating level-specific regressions ($\hat{\mathbf{B}}$), and (ii) constructing the optimal shrinkage hierarchy by optimizing ϕ .

The reformulation in Eq. 3.12 resembles a model-averaging estimator, where the models $\hat{\mathbf{B}}$ are averaged by the weights ϕ . Specifically, Mallows model averaging (MMA) represents a close mathematical pendant, where the weighting vector is obtained by minimizing the Mallows information criterion ([Hansen, 2007](#); [Mallows, 1973](#)). The optimal shrinkage problem of the HFR can correspondingly be thought of as the minimization of a custom information criterion (Eq. 3.11) to determine the optimal vector ϕ_λ^* (which, by extension, yields θ_λ^*). Since the objective of MMA is not shrinkage (despite the similar information theoretical motivation), it is not discussed in further detail here.⁴ Importantly, however, [Hansen \(2007\)](#) notes that the information theoretic model-averaging problem is quadratic in its weights (i.e. quadratic in ϕ), and can be solved ana-

⁴As a point of interest, the HFR could be formulated with appropriate (non-hierarchical) \mathbf{S} and \mathbf{H} matrices to reproduce the MMA estimator, however this represents a departure from the objective of a shrinkage estimator.

lytically using quadratic programming algorithms.

Following this line of reasoning, the level-specific coefficients in $\hat{\mathbf{B}}$ are used to define a quadratic program, with $\hat{\mathbf{y}} = \mathbf{x}\hat{\mathbf{B}}$, $\mathbf{U} = \frac{1}{2}\hat{\mathbf{y}}'\hat{\mathbf{y}}$ and $\mathbf{V} = \hat{\mathbf{y}}'y - \frac{N\lambda}{2}\boldsymbol{\nu}$, such that

$$\phi_\lambda^* = \arg \min_{\phi} [\phi' \mathbf{U} \phi - \mathbf{V}' \phi] \quad \text{s.t.} \quad \mathbf{0} \leq \phi' \boldsymbol{\omega} \leq \mathbf{1}. \quad (3.13)$$

Here $\boldsymbol{\nu}$ is an $L \times 1$ vector containing the number of nodes (ν_ℓ) in each level, with $\sum_\ell \nu_\ell = D$. Since the original shrinkage vector can be expressed as $\boldsymbol{\theta} = \phi' \boldsymbol{\omega}$, the constraint in Eq. 3.13 is identical to the constraint in Eq. 3.11.

Letting $\hat{\beta}_{qp;\phi_\lambda^*} = \hat{\mathbf{B}}\phi_\lambda^*$ be the vector of coefficients given by the average of the level-specific estimates, weighted by the optimal vector ϕ_λ^* , Proposition 2 asserts that $\hat{\beta}_{qp;\phi_\lambda^*}$ is equivalent to the optimal HFR coefficients $\hat{\beta}_{hfr;\theta_\lambda^*}$ obtained with θ_λ^* . This follows despite removing hierarchical path-dependence from $\hat{\mathbf{B}}$. A proof of Proposition 2 is given in Appendix C.

Proposition 2. *Let $\boldsymbol{\theta}$ be a vector of shrinkage weights, and $\hat{\beta}_{hfr;\theta}$ be the corresponding coefficients obtained by substituting $\boldsymbol{\theta}$ into Eq. 3.9. Furthermore, let ϕ be a transformation satisfying $\boldsymbol{\theta} = \phi' \boldsymbol{\omega}$ and $\boldsymbol{\omega}$ is an $L \times L$ lower triangular matrix, and let $\hat{\beta}_{qp;\phi} = \hat{\mathbf{B}}\phi$ be the corresponding coefficient vector.*

Now it holds that $\hat{\beta}_{qp;\phi_\lambda^} = \hat{\beta}_{hfr;\theta_\lambda^*}$, where θ_λ^* is the vector of shrinkage weights that minimizes the loss function of the HFR in Eq. 3.11 for any given λ , and ϕ_λ^* is the vector of transformed shrinkage weights defined in Eq. 3.13 for any given λ .*

The result in Proposition 2 is convenient, since it permits the HFR to embed both a parsimonious hierarchy, optimally shrinking individual levels of \mathbf{S} , as well as the corresponding coefficients, using a non-recursive estimation algorithm that performs L level-specific OLS regressions (to produce $\hat{\mathbf{B}}$) and a quadratic program (yielding ϕ_λ^*). In addition, formulating the problem in this manner permits parallel computation of level-specific regressions, as well as several flexible transformations of the shrinkage mechanism, such as the supervised factor regression proposed in Section 6.

The discussion up to this point has assumed a given hierarchy, encoded in \mathbf{S} . The aim of the HFR is to estimate \mathbf{S} in a supervised manner, which conceptually requires selecting the composition of predictor groups at each level that minimizes Eq. 3.11. This is a computationally intractable

combinatorial problem. Instead, the following section suggests a feasible and computationally efficient algorithm for arriving at a hierarchy based on the similarity of the predictors' explanatory structure in y .

3.5. Estimating the hierarchy

An important element of the HFR is the arrangement of predictors into an optimal hierarchical representation with nested disjoint subsets. An algorithm to estimate the hierarchy can be distilled to the questions of (i) how many subsets of variables to include at each individual level, and (ii) which predictors to cluster into these subsets.

The first question can be addressed in the framework described in Sections 3.3 & 3.4. By including $L = K$ levels, with each level containing exactly one more subset than the preceding level, the hierarchy spans the maximum number of non-overlapping levels possible. The first level, $\ell = 1$, contains exactly one cluster (the root node), while the final level, $\ell = L$, contains exactly K clusters (the leaf nodes). For the simple example in Section 3.2, there are $K = 4$ possible level configurations ($\ell = 3$ is ignored in the previous discussion):

$$\mathbf{S}_1 = \begin{bmatrix} 1 & 1 & 1 & 1 \end{bmatrix} \quad \mathbf{S}_2 = \begin{bmatrix} 1 & 1 & 0 & 0 \\ 0 & 0 & 1 & 1 \end{bmatrix} \quad \mathbf{S}_3 = \begin{bmatrix} 1 & 0 & 0 & 0 \\ 0 & 1 & 0 & 0 \\ 0 & 0 & 1 & 1 \end{bmatrix} \quad \mathbf{S}_4 = \begin{bmatrix} 1 & 0 & 0 & 0 \\ 0 & 1 & 0 & 0 \\ 0 & 0 & 1 & 0 \\ 0 & 0 & 0 & 1 \end{bmatrix}.$$

A parsimonious hierarchy containing only those levels that provide meaningful group shrinkage targets is obtained by removing all unnecessary levels, i.e. by setting all respective $\theta_\ell = 0$. The framework presented in the preceding sub-sections is sufficiently flexible to perform this shrinkage and can be used to select a parsimonious hierarchy retaining only the optimal number of subsets at each level, with any unnecessary levels automatically discarded by the optimal shrinkage vector θ_λ^* .

Answering the second question, of how optimally to cluster variables into subsets within each level, requires a combinatorial optimization over an exhaustive set of feasible groupings — a prohibitively complex task. For instance, in the case of \mathbf{S}_2 there are three possible groupings:

$$\mathbf{S}_2 = \left\{ \begin{bmatrix} 1 & 1 & 0 & 0 \\ 0 & 0 & 1 & 1 \end{bmatrix} \quad \begin{bmatrix} 0 & 1 & 1 & 0 \\ 1 & 0 & 0 & 1 \end{bmatrix} \quad \begin{bmatrix} 1 & 0 & 1 & 0 \\ 0 & 1 & 0 & 1 \end{bmatrix} \right\}.$$

In order to arrive at a workable method of selecting the optimal composition of subsets at each level, I propose the use of a supervised hierarchical clustering algorithm. Hierarchical clustering algorithms place similar predictors into clusters based on a measure of distance between predictors. Unlike other clustering algorithms, hierarchical clustering results in nested subsets, and is thus particularly well-suited for the current setting. A typical approach to hierarchical clustering constructs a dissimilarity matrix \mathbf{D} that encodes information about the predictor set (e.g. the (inverse) pairwise correlation coefficient of predictors), and calculates distances based on \mathbf{D} .

Such an approach is inherently unsupervised as it discards information about the correlation between \mathbf{x} and y . For a supervised solution, \mathbf{D} must capture the similarity of the explanatory portion of each predictor in \mathbf{x} , which encapsulates both the correlation structure of predictors, as well as the correlation between predictors and output. A suitable metric is the partial correlation coefficient $r_{x_i,y|x_{-i}}$, which measures the similarity between each predictor and the output conditional on all remaining predictors. The partial correlation cannot be computed without estimating the high-dimensional regression of y on \mathbf{x}_{-i} , which — in the context of regularized regression tasks — is at best imprecise, and at worst unfeasible if $K > N - 1$.

To solve this problem, a supervised dissimilarity matrix \mathbf{D}_y is defined, which captures the bivariate partial correlations with

$$\mathbf{D}_y = \{r_{x_i,y|x_j}\}_{i,j=1,\dots,K}, \quad \text{and} \quad r_{x_i,y|x_j} = \frac{r_{y,x_i} - r_{y,x_j}r_{x_i,x_j}}{\sqrt{(1 - r_{y,x_j}^2)(1 - r_{x_i,x_j}^2)}}, \quad i \neq j. \quad (3.14)$$

Clustering is then performed on a distance representation \mathbf{A}_y , computed as the Euclidean distance between rows in \mathbf{D}_y :

$$\mathbf{A}_y = \{a_{ij}\}_{i,j=1,\dots,K} \quad \text{with} \quad a_{ij} = \|\mathbf{d}_i - \mathbf{d}_j\|_2, \quad (3.15)$$

where \mathbf{d}_i and \mathbf{d}_j are rows in \mathbf{D}_y . Thus, while partial correlations are not computed in a fully conditional space, the approach clusters predictors based on the similarity of their bivariate partial

correlation profile. The hierarchical clustering performed using \mathcal{A}_y therefore has a supervised character, and — to the best of the author’s knowledge — represents a novel contribution to the field of hierarchical clustering.

The matrix \mathcal{D}_y is sign invariant by design, in the sense that negatively correlated predictors that have a similar explanatory effect on y (albeit with opposite signs), are clustered adjacently. This is desired behavior, with shrinkage effectively performed towards absolute group target values. For the final parameter estimates to reflect the correct sign, this invariance is corrected by adjusting the hierarchy summing matrix \mathbf{S} , altering the signs of predictors in each cluster to ensure only positive bivariate correlations among the variables in one cluster. Letting \mathbf{S}_i be a row in \mathbf{S} ,

$$\mathbf{S}_i = \mathbf{S}_i^+ \odot \text{sign}(\bar{\boldsymbol{\rho}}_i), \quad \bar{\boldsymbol{\rho}}_i = \mathbf{1}' \hat{\boldsymbol{\rho}}_{s_i} - \mathbf{1}, \quad (3.16)$$

where $\hat{\boldsymbol{\rho}}_{s_i}$ is the submatrix of $\hat{\boldsymbol{\rho}} = \text{cor}(\mathbf{x})$ containing the rows and columns where $\mathbf{S}_i^+ = 1$, and $\mathbf{1}$ is a vector of ones. The matrix \mathbf{S}^+ is the unadjusted (positive-only) summing matrix.

The distance matrix \mathcal{A}_y is clustered using a hierarchical clustering algorithm to generate an estimate of \mathbf{S}^+ . This class of algorithms recursively partitions elements in either a top-down (e.g. divisive analysis) or bottom-up (e.g. single linkage agglomerative nesting) manner, based on a distance representation of the input vectors (Maimon & Rokach, 2010). An exhaustive comparison of available algorithms is beyond the scope of this paper and is generally found to yield only minor differences for the performance of the HFR. The applications and simulations presented in subsequent sections employ complete linkage agglomerative nesting, which generally constructs more homogeneous and evenly sized clusters compared to the alternatives (Everitt *et al.*, 2011).

A description of complete linkage agglomerative nesting can be found in Kaufman & Rousseeuw (2005) and Everitt *et al.* (2011). The algorithm begins by placing each column vector in \mathcal{A}_y into a cluster of its own, and iteratively merges the clusters with the minimum cluster distance to form new levels. Clusters are merged a total of $K - 1$ times, until all columns in \mathcal{A}_y are contained in a single cluster, and $L = K$ levels have been formed. The distance between two clusters is defined as the maximum Euclidean distance between any two column vectors contained within the respective clusters. The algorithm is implemented using the `cluster` package in the statistical computing language R (Maechler *et al.*, 2019; R Core Team, 2018).

3.6. Adding a constant

The preceding discussions have abstracted from deterministic elements in the regression. Including these is exceedingly simple, and can be achieved by adjusting the level-specific regressions in $\hat{\mathcal{B}}$. Letting $\mathbf{m} = \{\mathbf{m}_i\}_{i=1,\dots,N} \in \mathbb{R}_M$ be a matrix of M deterministic elements (e.g. a constant), the level-specific regression becomes:

$$\hat{\mathbf{w}}_\ell = \tilde{\mathbf{S}}_\ell' (\tilde{\mathbf{z}}_\ell' \tilde{\mathbf{z}}_\ell)^{-1} \tilde{\mathbf{z}}_\ell' \mathbf{y}, \quad (3.17)$$

where $\tilde{\mathbf{z}}_\ell = \begin{bmatrix} \mathbf{m} & \mathbf{z}_\ell \end{bmatrix}$, and $\tilde{\mathbf{S}}_\ell$ expands \mathbf{S}_ℓ such that

$$\tilde{\mathbf{S}}_\ell = \begin{bmatrix} \mathbf{I}_M & \mathbf{0} \\ \mathbf{0} & \mathbf{S}_\ell \end{bmatrix}.$$

Since deterministic elements are exogenous to the estimation of the hierarchy, the corresponding parameters are not regularized towards group targets. Apart from a regression constant, deterministic elements can include statistical features such as trends or dummy variables, or simply predictors that, for one reason or another, are better represented outside of the feature hierarchy. All applications in this paper contain a deterministic element in the form of a regression constant.

4. Simulations

In the following sections, the predictive performance of the HFR is examined, first in a simulated and then in an empirical environment. I use four simulations, largely replicated from related work, that cover different types of regression tasks to compare the performance of the HFR to similar methods. The benchmark methods include penalized regressions in the form of the ridge regression, Lasso, Adaptive Lasso (AdaLasso) and ElasticNet, latent variable regressions in the form of PCR and PLSR, and finally OLS.⁵

The simulations show that each benchmark method is particularly well suited to certain regression tasks and poorly to others, as is generally observed in the related literature (Tibshirani, 1996). The

⁵Ridge, Lasso and ElasticNet are implemented using the `glmnet`-package in the statistical computing language R, described in Friedman *et al.* (2010). For a discussion of the AdaLasso, see Zou (2006). PLSR is implemented using the `pls`-package in the statistical computing language R, described in Mevik & Wehrens (2019).

HFR, by contrast, exhibits a high degree of versatility, outperforming or matching the benchmark methods in all simulations. Three of the simulations are based on [Tibshirani \(1996\)](#) and [Zou & Hastie \(2005\)](#) and have been applied occasionally in similar research ([Bondell & Reich, 2008](#)). The final simulation is new.

Data is simulated from the true model

$$y = \mathbf{x}\boldsymbol{\beta} + \epsilon, \quad \epsilon \sim \mathcal{N}(0, \sigma^2).$$

Observations are divided into training, validation and testing samples, where the training sample is used to estimate the models, the validation sample is used to determine optimal hyperparameters, and the testing sample is used for performance evaluation. Model performance is assessed by calculating the mean squared error (MSE) over the testing sample. Sample sizes are denoted by $\cdot/\cdot/\cdot$, where the dots represent training, validation and testing samples, respectively. In each case, the results of 100 simulation runs are plotted.

Hyperparameters include the size of the penalty (λ) for the penalized estimators (ridge, Lasso, AdaLasso, ElasticNet and HFR), and the mixing parameter (α) for the ElasticNet. The PCR and PLSR estimate latent factors, which are used to generate predictions. The number of latent factors (components) to include in the regressions is also determined using the validation sample, by treating it as a hyperparameter. Optimal hyperparameter values are determined using an extensive grid search with selection based on the minimum validation MSE. Hyperparameter tuning is performed individually for each method in each simulation run.

4.1. *Simulation setup*

Simulation (a) is taken from [Tibshirani \(1996\)](#), where it was originally used to demonstrate the performance of the ridge regression. True parameter values are set to $\beta_j = 0.85, \forall j = 1, \dots, K$, with $K = 8$. The sample size is 20/20/200, $\sigma^2 = 3$ and the pairwise correlation between x_i and x_j is $0.5^{|i-j|}$.

Simulation (b) is again based on [Tibshirani \(1996\)](#) and is a sparse regression used to illustrate

the Lasso's ability of eliminating noise features. There are 40 predictors with parameters set to

$$\boldsymbol{\beta} = (\underbrace{0, \dots, 0}_{10}, \underbrace{2, \dots, 2}_{10}, \underbrace{0, \dots, 0}_{10}, \underbrace{2, \dots, 2}_{10}).$$

As before the pairwise correlation between x_i and x_j is $0.5^{|i-j|}$, and $\sigma^2 = 15$. The sample size is set to 100/100/400. Since the DGP is sparse, the task is likely to be solved well with a Lasso, AdaLasso or ElasticNet. Variations on this simulation are used in Section 4.4 to explore scenarios for which the HFR is less suitable.

Simulation (c) is taken from [Zou & Hastie \(2005\)](#), who study the effect of grouped predictors. The simulation contains a mixture of grouped predictors and noise predictors and is therefore a grouped feature selection task. The sample consists of 50/50/400 observations and 40 predictors with

$$\boldsymbol{\beta} = (\underbrace{3, \dots, 3}_{15}, \underbrace{0, \dots, 0}_{25}),$$

$\sigma^2 = 15$, and \mathbf{x} generated as follows (with $\epsilon_i^x \sim \mathcal{N}(0, 0.01)$):

$$\begin{aligned} x_i &= \xi_1 + \epsilon_i^x, \quad \xi_1 \sim \mathcal{N}(0, 1), \quad i = 1, \dots, 5 \\ x_i &= \xi_2 + \epsilon_i^x, \quad \xi_2 \sim \mathcal{N}(0, 1), \quad i = 6, \dots, 10 \\ x_i &= \xi_3 + \epsilon_i^x, \quad \xi_3 \sim \mathcal{N}(0, 1), \quad i = 11, \dots, 15 \\ x_i &\sim \mathcal{N}(0, 1), \quad i = 16, \dots, 40. \end{aligned}$$

The noise features are generated with a pairwise correlation of 0.3. The simulation is designed to illustrate the ability of the ElasticNet to deal with grouped variables and variable selection simultaneously, and should therefore see the ElasticNet performing well.

Simulation (d) is designed to test predictive performance in the presence of latent factors. The sample consists of 20/20/200 observations. Simulation (d) draws from a true model $y = \mathbf{f}\boldsymbol{\beta} + \epsilon$ where $\mathbf{f} = [f_1 \ \dots \ f_4]$, $\boldsymbol{\beta} = (1.0, 1.5, 2.0, 1.5)$, $\sigma^2 = 3$ and the pairwise correlation between f_i and f_j is $0.5^{|i-j|}$. Unlike the previous cases, I assume \mathbf{x} contains noisy measures of the unobserved

latent factors \mathbf{f} , such that (with $\epsilon_i^x \sim \mathcal{N}(0, 1)$):

$$x_i = f_1 + f_2 + \epsilon_i^x, \quad i = 1, 2$$

$$x_i = f_2 + f_3 + \epsilon_i^x, \quad i = 3, 4$$

$$x_i = f_3 + f_4 + \epsilon_i^x, \quad i = 5, 6$$

$$x_i = f_4 + f_1 + \epsilon_i^x, \quad i = 7, 8$$

The PCR is expected to outperform other regularized regressions in this example.

4.2. Simulation results

Figure 4.1 plots the model accuracy for Simulations (a) to (d). The HFR outperforms the benchmarks in all simulations. Good performance in the cases when no predictor groups exist in the true DGP (Simulations (a) & (b)), or when an overlapping grouping structure exists (Simulation (d)) illustrate the versatility of the HFR in estimating robust parameters. The feature selection tasks (Simulations (b) & (c)) demonstrate how the ability of grouping noise features can lead to good performance even when compared to methods that explicitly perform variable selection, such as the Lasso, AdaLasso and ElasticNet regressions.

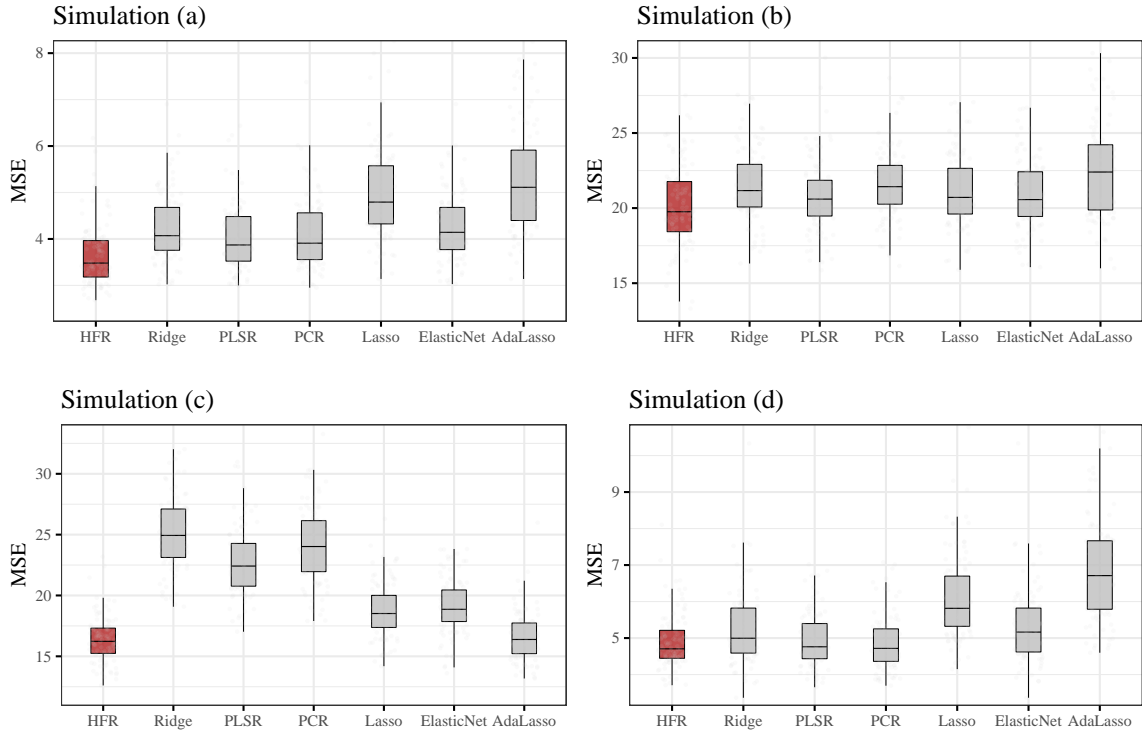


Figure 4.1: Comparison of prediction accuracy of hierarchical feature regression (HFR), Ridge, PLSR, PCR, ElasticNet, Lasso and AdaLasso for simulations (a)-(d).

The average comparative rank of the different estimators is plotted in Figure 4.2 and suggests a highly favorable relative performance of the HFR, with the lowest mean rank achieved in each instance. The figure is useful in uncovering relative performance attributes not easily discerned in Figure 4.1, such as the superior accuracy of the ElasticNet in Simulation (b) in relation to other feature selection algorithms like Lasso or AdaLasso, and provides additional evidence of the accuracy and versatility of the HFR.

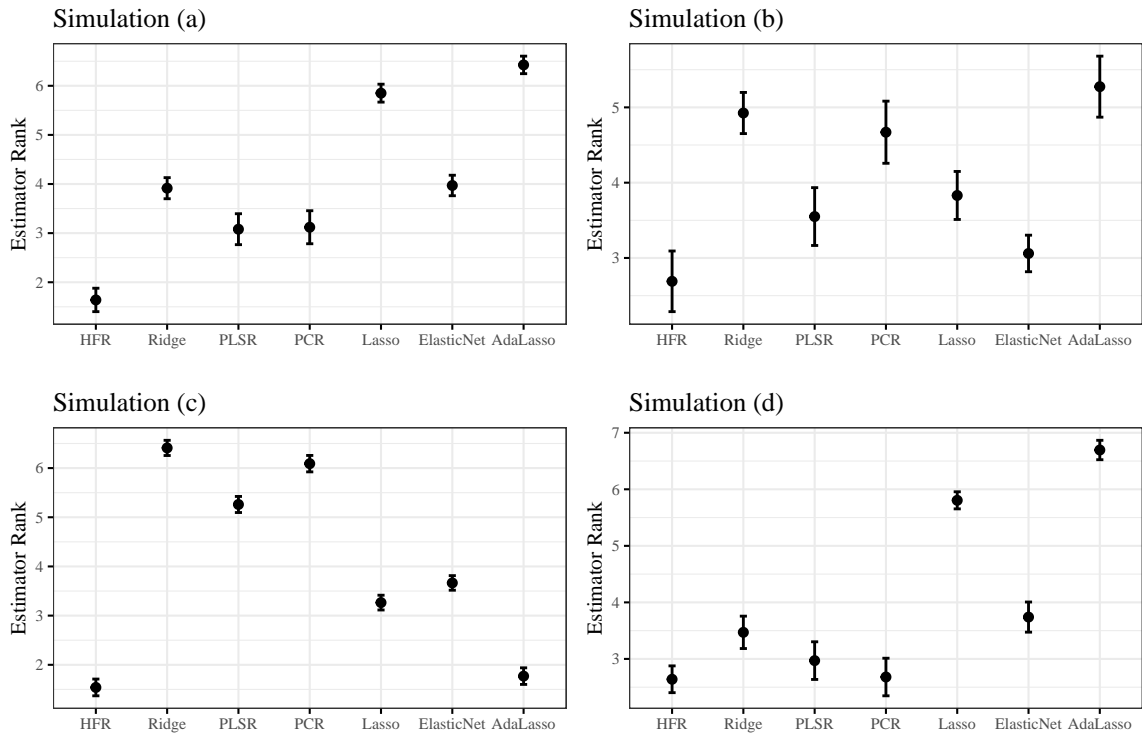


Figure 4.2: Comparison of average predictor rank by MSE of HFR, Ridge, PLSR, PCR, ElasticNet, Lasso and AdaLasso for simulations (a)-(d). Mean and 95% confidence interval from 100 simulation runs are plotted.

Table 4.1 summarizes the results of the simulations including bootstrap standard errors for the median MSE performance metrics:

	Sim. (a)	Sim. (b)	Sim. (c)	Sim. (d)
HFR	3.481 (0.122)	19.757 (0.333)	16.23 (0.233)	4.705 (0.083)
Ridge	4.07 (0.08)	21.167 (0.267)	24.934 (0.311)	4.995 (0.113)
PLSR	3.871 (0.063)	20.599 (0.269)	22.417 (0.386)	4.761 (0.082)
PCR	3.909 (0.069)	21.428 (0.341)	24.023 (0.479)	4.717 (0.066)
Lasso	4.793 (0.159)	20.713 (0.26)	18.516 (0.202)	5.814 (0.126)
ElasticNet	4.143 (0.088)	20.568 (0.192)	18.862 (0.207)	5.164 (0.092)
AdaLasso	5.112 (0.15)	22.404 (0.495)	16.383 (0.262)	6.711 (0.17)
OLS	5.138 (0.183)	25.13 (0.65)	86.929 (4.017)	7.396 (0.31)

Table 4.1: Prediction accuracy (median MSE) for simulations (a)-(d) based on 100 simulation runs. Standard errors in parentheses. Standard errors are calculated using 500 bootstrap resamplings of the estimated MSE. In each case the two best methods are highlighted.

4.3. Trace plots

In order to explore shrinkage behavior in the HFR, Fig. 4.3 draws trace plots of $\hat{\beta}_{\text{hfr}}$, using the setup in Simulation (a), with $K = 8$ predictors. The plot illustrates, how parameter estimates are drawn towards group targets at differing rates depending, roughly, on the extent of their average bilateral correlation, with all parameters included in a single group as λ increases. The estimates are eventually shrunken towards zero for large λ values.

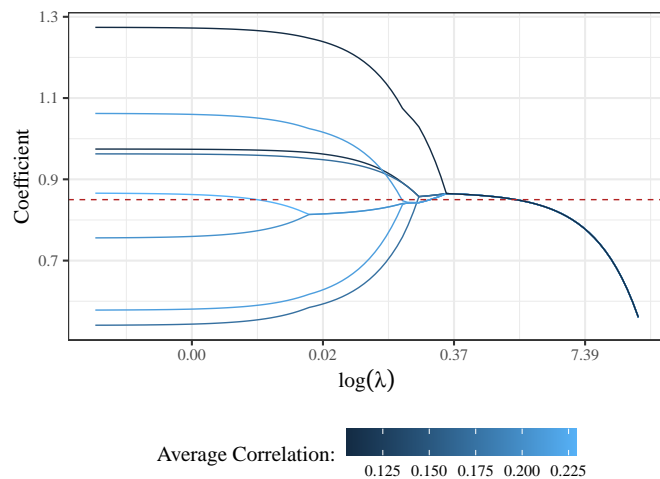


Figure 4.3: HFR trace plots for $K = 8$ predictors. Average bilateral correlation of the variables is represented by the color. True parameter values are represented by the dashed line.

By way of comparison, Fig. 4.4 draws trace plots for the ridge regression and Lasso estimators using the same regression problem as above. The plots highlight the key difference between the HFR and traditional regularized regressions, which penalize the parameter norm and reduce all coefficient estimates towards zero. The HFR can reduce noise in a highly efficient manner, with only limited attenuation bias in the estimates (see dashed line in Fig. 4.3). For the given regression problem, ridge and Lasso can only eliminate a meaningful portion of the noise at levels of λ that result in parameters estimated with substantial attenuation bias.

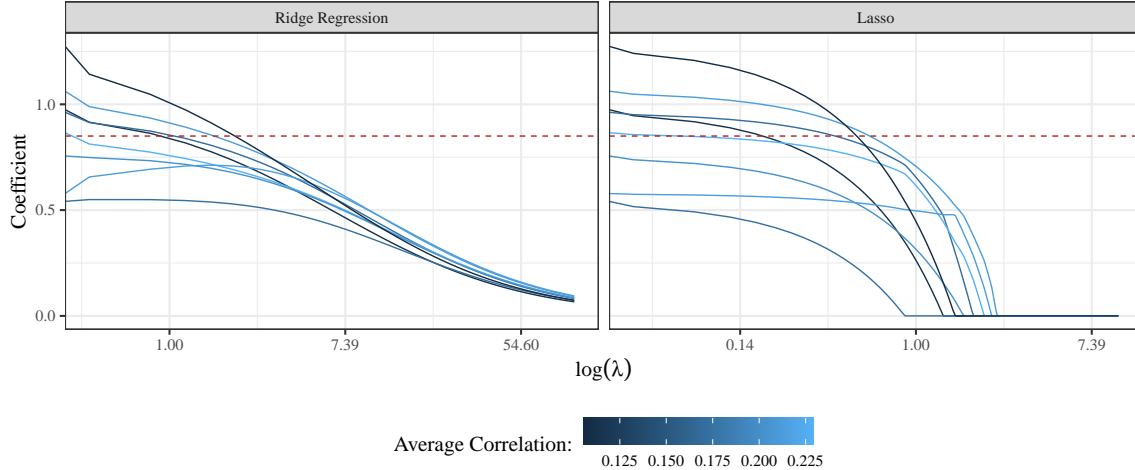


Figure 4.4: Trace plots of ridge regression and Lasso estimators for $K = 8$ predictors. Average bilateral correlation of the variables is represented by the color. True parameter values are represented by the dashed line.

4.4. Boundary cases

While the above results demonstrate the high degree of accuracy and versatility of the HFR, it can potentially yield less convincing outcomes in at least two scenarios, as illustrated in the following variations on Simulation (b):

Simulation (e) repeats Simulation (b), but with true parameters equal to

$$\beta = (\underbrace{0, \dots, 0}_{10}, \underbrace{1, \dots, 3}_{10}, \underbrace{0, \dots, 0}_{10}, \underbrace{-1, \dots, -3}_{10}).$$

Here the second and fourth parameter blocks represent evenly spaced sequences on the interval $[1, 3]$ and $[-3, -1]$, respectively. This requires the HFR to construct a shallower hierarchy, since the effect of the predictors on y is more heterogeneous and more idiosyncratic information must be included. A shallower hierarchy limits the feasible extent of regularization, and results in a higher effective degrees of freedom.

Simulation (f) is identical to Simulation (b), but with a pairwise correlation between x_i and x_j of 0.5. The high degree of correlation between noise and signal predictors results in an extremely noisy \mathcal{D}_y matrix that cannot be clustered in any meaningful manner. Thus, the HFR can only poorly distinguish between signal and noise predictors and hierarchy construction becomes essentially random.

The results are plotted in Fig. 4.5 and Table 4.2. In Simulation (e), the variability of all methods

increases, however, HFR again outperforms the benchmarks, suggesting that the method can achieve good out-of-sample results, even when the scope for shrinkage is reduced. In Simulation (f), the HFR exhibits an average performance, roughly on par with the PCR and PLSR, but worse than penalized regressions, suggesting that significant value is added by a meaningful clustering of predictors into hierarchical groups.

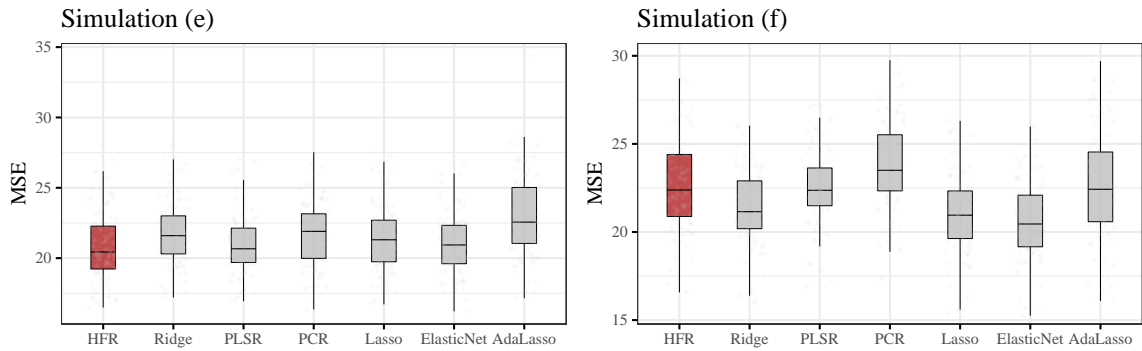


Figure 4.5: Comparison of prediction accuracy of hierarchical feature regression (HFR), Ridge, PLSR, PCR, ElasticNet, Lasso, and AdaLasso for simulations (e)-(f)

	Sim. (e)	Sim. (f)
HFR	20.44 (0.266)	22.384 (0.401)
Ridge	21.599 (0.255)	21.153 (0.226)
PLSR	20.667 (0.337)	22.367 (0.17)
PCR	21.904 (0.323)	23.5 (0.302)
Lasso	21.306 (0.372)	20.954 (0.235)
ElasticNet	20.936 (0.363)	20.453 (0.224)
AdaLasso	22.562 (0.39)	22.424 (0.379)
OLS	25.165 (0.357)	25.13 (0.65)

Table 4.2: Prediction accuracy (median MSE) for simulations (e)-(f) based on 100 simulation runs. Standard errors in parentheses. Standard errors are calculated using 500 bootstrap resamplings of the estimated MSE. In each case the two best methods are highlighted.

In sum, the simulations make a compelling case for the use of the HFR estimator. The versatility of the HFR across a spectrum of different types of regression tasks is a key strength when compared to the benchmarks, which are typically tailored to serve specific purposes. Whether these advantages translate well to a real-world empirical setting is explored in the following section using a widely applied data set of economic growth determinants.

5. Empirical application: Determinants of economic growth

In their seminal paper on the determinants of economic growth, [Sala-I-Martin *et al.* \(2004\)](#) compile a cross-country data set comprising GDP per capita growth rates between 1960-1996 for 88 countries, as well as 67 potential explanatory variables. The data set has been applied on multiple occasions, in attempts to derive the most important drivers of economic growth, and has become a workhorse data set to test high-dimensional regression techniques, particularly in the Bayesian literature ([Eicher *et al.*, 2011](#); [Hofmarcher *et al.*, 2011](#); [Ley, 2008](#); [Sala-I-Martin *et al.*, 2004](#); [Schneider & Wagner, 2012](#)). The econometric techniques employed include Bayesian model averaging, as well as Bayesian and frequentist applications of Lasso and ElasticNet estimators. A key consideration for the validity of the applied model is its predictive performance, which has been assessed by several authors.

In this section, I use the HFR to predict economic growth based on the 67 predictors contained in the data set of [Sala-I-Martin *et al.* \(2004\)](#) and compare the (pseudo) out-of-sample accuracy to the benchmarks used in Section 4, as well as Bayesian model averaging of [Sala-I-Martin *et al.* \(2004\)](#) (BACE), as replicated in [Hofmarcher *et al.* \(2011\)](#), and the Bayesian ElasticNet of [Hofmarcher *et al.* \(2011\)](#) (BEN).⁶ The HFR is found to outperform all Bayesian and non-Bayesian benchmarks in terms of predictive accuracy, and is capable of generating interesting additional insights into the latent forces that drive disparities in economic growth.

Since the HFR and the benchmark methods require the ranges of the input variables to be similar, the 67 predictors in the data set are scaled to an interval of $[-1, 1]$. Dummy variables are normalized to a range of $[-0.5, 0.5]$. This is done to dampen the effect of the dummy variables in the hierarchy, since the remaining variables only possess few observations at the extreme ends of their range, while the bulk of the density function lies within a narrower interval. The GDP per capita growth variable is not transformed to ensure that a comparison to previous research is possible.⁷ Furthermore, all specifications include an intercept.

The predictive performance is evaluated in a similar manner as in [Hofmarcher *et al.* \(2011\)](#). Observations are randomly sampled to form training, validation and testing samples containing 68/10/10, respectively.⁸ Parameters are estimated using the training sample, hyperparameters are

⁶These particular authors are selected because they present sufficiently detailed results to facilitate a comparison within the context of this analysis.

⁷Note that the variable is centered for the ridge, Lasso and ElasticNet analyses, but remains unscaled.

⁸These proportions are roughly equivalent to those used in [Hofmarcher *et al.* \(2011\)](#), but with the addition of a

determined via a grid search minimization of the validation MSE and the performance is calculated as the test sample MSE. Samples are drawn in 200 iterations with hyperparameters determined independently in each run.

Figure 5.1 plots the MSE and the average rank for the HFR and benchmark methods. In addition, Table 5.1 displays the distribution of the MSEs alongside the results of the BACE and the BEN. The estimation of BACE and BEN is not replicated, but the results are taken directly from the table presented in [Hofmarcher *et al.* \(2011\)](#), page 10.

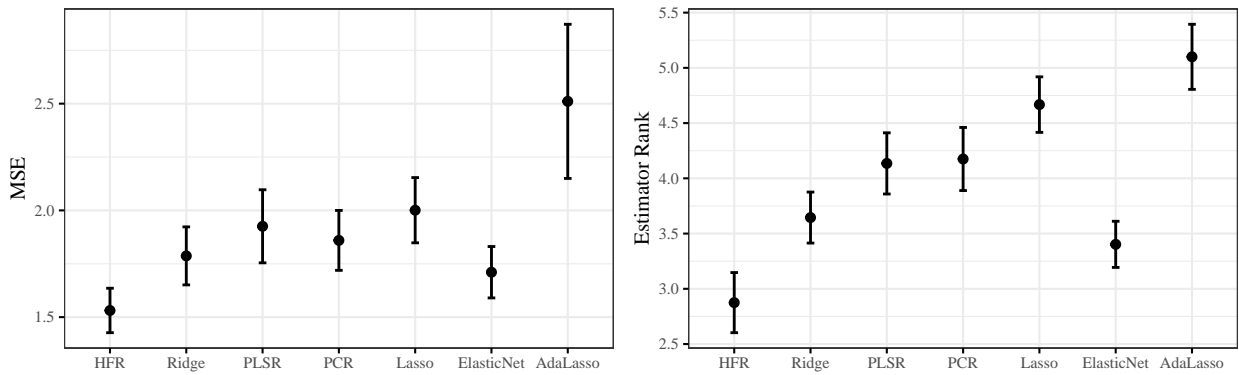


Figure 5.1: Comparison of prediction accuracy of HFR, Ridge, PLSR, PCR, ElasticNet, Lasso, and AdaLasso for GDP per capita growth from 1960-1996. MSE (left panel), rank of estimators (right panel). Statistics plotted as mean and 95% confidence interval based on 200 random training, validation and testing samples. Prediction errors are multiplied by 1e4.

	HFR	Ridge	PLSR	PCR	Lasso	ElasticNet	AdaLasso	BACE	BEN
Min.	0.239	0.144	0.340	0.301	0.309	0.138	0.192	0.358	0.452
1st Qu.	0.971	1.039	1.165	1.115	1.279	1.051	1.346	1.122	1.114
Median	1.320	1.628	1.668	1.640	1.821	1.495	2.104	1.614	1.494
Mean	1.531	1.787	1.926	1.860	2.001	1.710	2.511	1.705	1.587
3rd Qu.	2.075	2.328	2.443	2.352	2.490	2.194	3.043	2.158	1.869
Max.	4.241	5.255	12.868	5.908	8.868	5.273	28.042	4.213	3.891

Table 5.1: Distribution of prediction error (MSE) for GDP per capital growth based on 200 simulation runs. Prediction errors are multiplied by 1e4.

The HFR is found to outperform all benchmark methods, with the ElasticNet regression achieving the highest mean accuracy among the frequentist benchmarks in Fig. 5.1. Apart from attaining

validation sample, which is obtained by reducing the size of both the training and testing samples slightly.

lower mean and median prediction errors, the HFR also exhibits lower variation in the MSE. When compared to the performance of the BACE and BEN models, the HFR is again found to achieve lower mean and median prediction errors. None of the frequentist benchmarks outperform the Bayesian BACE or BEN models. The favorable results provide an indication that the performance of the HFR, observed in the simulations, translates well to the empirical setting.

A study of the coefficients estimated by the HFR for the 67 predictors provides interesting insights into the mechanics underpinning the regularized regression. Fig. 5.2 plots the coefficients estimated in each of the 200 runs (boxplot) overlaid by the OLS coefficients (crosses). The regularized coefficients differ substantially from the OLS estimates (which appear nonsensical in many cases) and agree broadly with the findings of [Sala-I-Martin *et al.* \(2004\)](#) and [Hofmarcher *et al.* \(2011\)](#). The highlighted boxes represent the most important determinants of economic growth uncovered by the BACE process in [Sala-I-Martin *et al.* \(2004\)](#) or the BEN in [Hofmarcher *et al.* \(2011\)](#), and correspond in most instances to the largest coefficients estimated by the HFR. A large number of coefficients are reduced to values close to zero, demonstrating a manner of variable selection performed by the HFR. Note that the fact that predictors are normalized to a similar range permits approximate comparison of the coefficient magnitudes. A description of the predictors included in the data set can be found in Table 5.2.

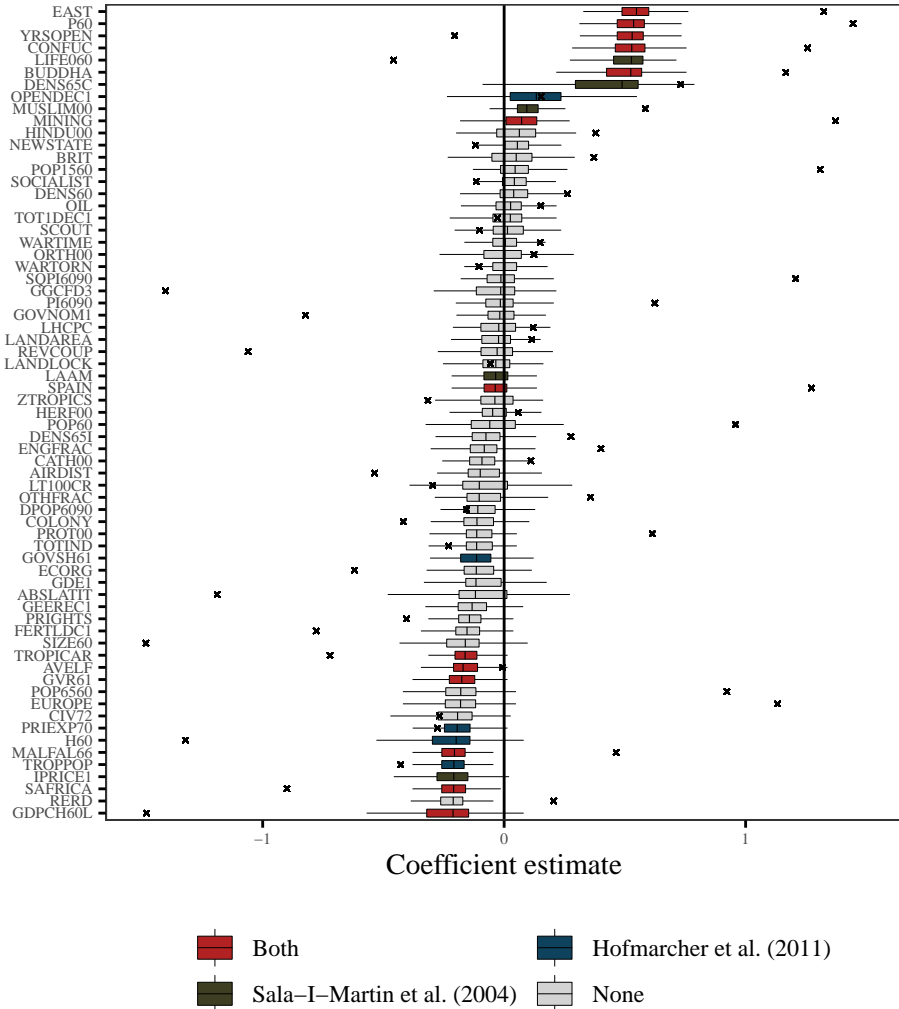


Figure 5.2: HFR coefficients of growth determinants for 200 random sub-samples. Points represent full sample OLS estimates. The color indicates inclusion in the set of most important determinants of economic growth from Sala-I-Martin et al. (2004), Hofmarcher et al. (2011), or both.

There are several approaches that can be used to explore how groups of variables are regularized in the HFR.⁹ One approach is to examine the most important nodes in the hierarchical feature space. The node-specific weights (after applying optimal shrinkage) are given by

$$\hat{\beta}_{\text{hfr}}^\dagger = (\mathbf{z}' \mathbf{z} \odot \mathbf{H} \odot \boldsymbol{\Theta})^{-1} \mathbf{z}' \mathbf{y}, \quad (5.1)$$

⁹Apart from examining node-specific weights — discussed in this section —, another approach to exploring regularization uses the factor rotation matrix introduced in Section 6.1, which contains loading coefficients of each HFR parameter on each OLS parameter. The absolute size of the loadings represents a useful summary of regularization and clustering in the HFR.

where $\hat{\beta}_{\text{hfr}} = \mathbf{S}'\hat{\beta}_{\text{hfr}}^\dagger$ and Θ is constructed using θ_λ^* . Each element in $\hat{\beta}_{\text{hfr}}^\dagger$ represents the weight given to the common factor defined by the corresponding row in \mathbf{S} . Examining the clusters associated with the largest node-specific weights (where the weights are normalized by the fraction of variables contained in each respective node to make them comparable), can potentially unearth deeper hierarchical factors that drive economic growth.

Fig. 5.3 plots a hierarchy dendrogram for the model, highlighting the three most important clusters of variables (i.e. the nodes with the largest normalized node-specific weights). The common explanatory information contained in these groups of variables is a key empirical determinant of growth. The first group contains variables associated with East Asian economies (e.g. BUDDHA, CONFUC, EAST), the second, variables presumably associated with African economies (e.g. MALFAL66, SAFRICA, TROPPOP), while the third group contains variables likely to be associated with European economies (e.g. EUROPE, CIV72, POP6560, ECORG). The variables in the first group all enter with positive regression coefficients, while the variables in the second and third groups all enter with negative coefficients (see Fig. 5.2).

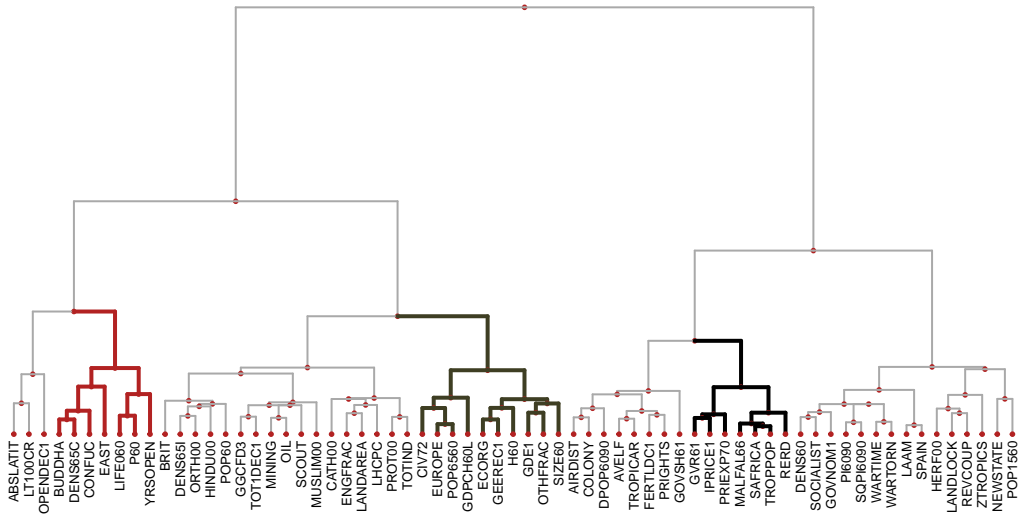


Figure 5.3: Hierarchy dendrogram for the optimal HFR estimates. The optimal degree of shrinkage is determined using a 10-fold cross-validation with similar proportions as in the simulation above. The three most important clusters in the hierarchy are highlighted.

Together, the three groups explain a large portion of the variation captured by the HFR (the R^2 statistic of the HFR estimates is 0.73, while the portion explained by the three top clusters is

0.68).¹⁰ The importance of the clusters in Fig. 5.3 provides evidence for the existence of a broader Asian factor that explains high growth instances, and broader African and European factors that explain low growth instances. The fact that the upper clusters enter with a much higher importance than their corresponding leaf nodes, suggests that the common — as opposed to the idiosyncratic — information in the predictor groups determines growth disparities. For instance, rather than malaria prevalence entering as a growth determinant in its own right, the variable (MALFAL66) helps to identify an underlying geographic factor that drives economic growth.

Fig. 5.4 plots traces for the first and second variable groups, visualizing the effect of the penalty. The left panel displays variables closely associated with Asian economies, while the right panel groups variables related to African economies. Note that variables such as population density and life expectancy are arranged into the East Asian cluster, while economic variables such as IPRICE1 and RERD are arranged into the African cluster. Parameters are generally regularized towards common means at differing paces, with fewer group targets as λ increases. Eventually, all estimates collapse into a single mean, which is regularized towards zero for very large values of λ .

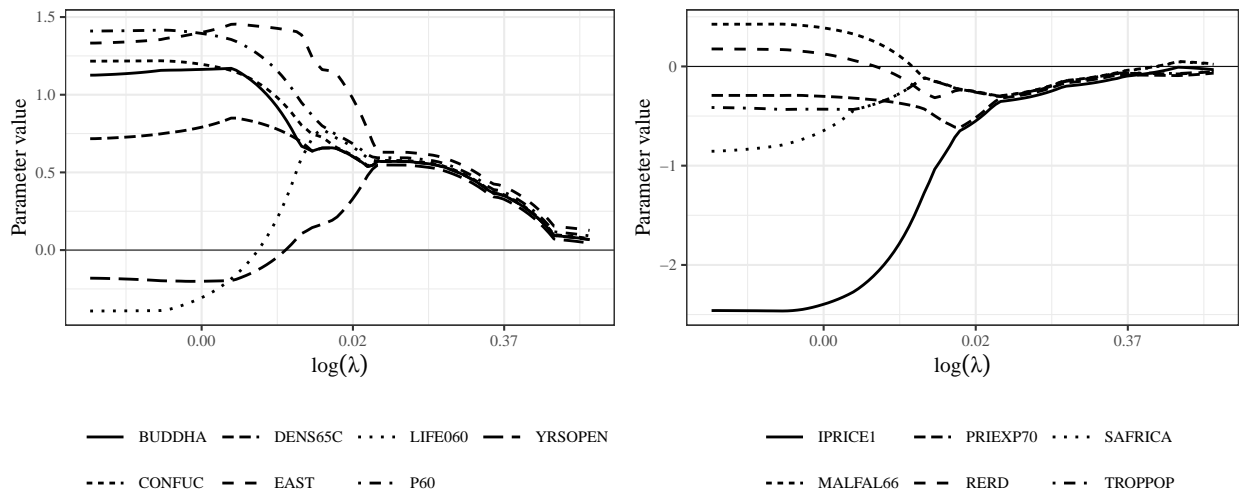


Figure 5.4: Trace plots for the variables contained in the East Asia and Africa clusters. The variable GVR61 is omitted from the right panel plot, due to its extremely large size when the problem is not or only mildly regularized.

Apart from producing robust out-of-sample predictions, the parsimonious hierarchy, in which HFR estimates are embedded, allows for the emergence of meta-insights about the importance of the underlying latent signals that explain observed response variation. In the case of the determinants

¹⁰The explained variation of the three top clusters is calculated as the coefficient of determination of a regression including only the factors associated with these clusters.

of economic growth, three factors — identifying regional sub-clusters — may suffice to offer robust explanations of observed growth disparities. This ability to distinguish between the types of explanatory variation (shared or idiosyncratic) within a fully supervised framework is unique to the HFR, and can provide valuable additional insight with respect to the data generating process. For instance, in the context of the current application, the findings suggest that the question of discovering individual growth determinants is misplaced, or needs to be performed only after controlling for regional or geographic factors.

Description	Name	Description	Name
Absolute Latitude	ABSLATIT	Fraction of Land Area Near Navigable Water	LT100CR
Air Distance to Big Cities	AIRDIST	Malaria Prevalence in 1960s	MALFAL66
Ethnolinguistic Fractionalization	AVELF	Fraction GDP in Mining	MINING
British Colony Dummy	BRIT	Fraction Muslim	MUSLIM00
Fraction Buddhist	BUDDHA	Timing of Independence	NEWSTATE
Fraction Catholic	CATH00	Oil Producing Country Dummy	OIL
Civil Liberties	CIV72	Openness measure 1965-74	OPENDEC1
Colony Dummy	COLONY	Fraction Orthodox	ORTH00
Fraction Confucian	CONFUC	Fraction Speaking Foreign Language	OTHFRAC
Population Density 1960	DENS60	Primary Schooling in 1960	P60
Population Density Coastal in 1960s	DENS65C	Average Inflation 1960-90	PI6090
Interior Density	DENS65I	Square of Inflation 1960-90	SQPI6090
Population Growth Rate 1960-90	DPOP6090	Political Rights	PRIGHTS
East Asian Dummy	EAST	Fraction Population Less than 15	POP1560
Capitalism	ECORG	Population in 1960	POP60
English Speaking Population	ENGFRAC	Fraction Population Over 65	POP6560
European Dummy	EUROPE	Primary Exports 1970	PRIEXP70
Fertility in 1960s	FERTLDC1	Fraction Protestants	PROT00
Defense Spending Share	GDE1	Real Exchange Rate Distortions	RERD
GDP in 1960 (log)	GDPCH60L	Revolutions and Coups	REVCOUP
Public Education Spending Share in GDP in 1960s	GEEREC1	African Dummy	SAFRICA
Public Investment Share	GGCFD3	Outward Orientation	SCOUT
Nominal Government GDP Share 1960s	GOVNOM1	Size of Economy	SIZE60
Government Share of GDP in 1960s	GOVSH61	Socialist Dummy	SOCIALIST
Gov. Consumption Share 1960s	GVR61	Spanish Colony	SPAIN
Higher Education 1960	H60	Terms of Trade Growth in 1960s	TOT1DEC1
Religion Measure	HERF00	Terms of Trade Ranking	TOTIND
Fraction Hindus	HINDU00	Fraction of Tropical Area	TROPICAR
Investment Price	IPRICE1	Fraction Population In Tropics	TROPOPOP
Latin American Dummy	LAAM	Fraction Spent in War 1960-90	WARTIME
Land Area	LANDAREA	War Participation 1960-90	WARTORN
Landlocked Country Dummy	LANDLOCK	Years Open 1950-94	YRSOPEN
Hydrocarbon Deposits in 1993	LHCPC	Tropical Climate Zone	ZTROPICS
Life Expectancy in 1960	LIFE060		

Table 5.2: Description of growth determinants included in the dataset of Sala-I-Martin et al. (2004)

6. Future work and extensions

6.1. HFR as a factor regression

The formulation of the HFR as a quadratic program in Eq. 3.13 allows for an interesting extension. By replacing the penalty $\lambda\nu$ with an explicit constraint on $\phi'\nu$, the HFR can be estimated with an exact specification of the number of effective degrees of freedom. Instead of the hyperparameter λ governing the size of the penalty, a hyperparameter η is introduced, which can be interpreted as the effective degrees of freedom of the model (with $\eta = \text{tr}(\mathbf{P}_{\text{hfr}})$ by construction). The quadratic program becomes

$$\phi_\eta^* = \arg \min_{\phi} [\phi' \mathbf{U} \phi - \mathbf{V}' \phi] \quad \text{s.t.} \quad \mathbf{0} \leq \phi' \omega \leq 1 \text{ and } \phi' \nu = \eta, \quad (6.1)$$

where $\mathbf{V} = \frac{2}{N} \hat{\mathbf{y}}' \mathbf{y}$ and $\mathbf{U} = \frac{1}{N} \hat{\mathbf{y}}' \hat{\mathbf{y}}$. Here η represents the constraint on the degrees of freedom, with $\eta = K$ resulting in the unregularized OLS estimates. Importantly, using the hyperparameter η instead of λ does not affect the estimate values, or the performance of the estimator, but simply reformulates the estimator from a penalized regression to a factor regression.

When $\eta < K$, the HFR is analogous to a principal components regression with η underlying principal components. However, in the case of the HFR, the statistical components are estimated in a fully supervised framework, where the factor construction and regression steps cannot be separated as in a PCR. Furthermore, η can take on any real value with $0 \leq \eta \leq K$, and is not limited to integers.

The factor loading matrix implied by the HFR can be calculated as:

$$\boldsymbol{\Gamma} = \mathbf{S}' (\mathbf{z}' \mathbf{z} \odot \mathbf{H} \odot \boldsymbol{\Theta})^{-1} \mathbf{z}' \mathbf{x}. \quad (6.2)$$

$\boldsymbol{\Gamma}$ encapsulates the hierarchical rotation of the parameter space, with $\hat{\boldsymbol{\beta}}_{\text{hfr}} = \boldsymbol{\Gamma} \hat{\boldsymbol{\beta}}_{\text{ols}}$. This transformation satisfies Eq. 6.3:

$$\hat{\boldsymbol{\beta}}_{\text{hfr}} = (\boldsymbol{\Phi}' \boldsymbol{\Phi})^{-1} \boldsymbol{\Phi}' \mathbf{y}, \quad (6.3)$$

where $\Phi = \mathbf{x}\boldsymbol{\Gamma}^{-1}$ are the factors generated by the hierarchical rotation. Unlike in the case of a principal components regression, the dimensions of the factor matrix are not reduced (i.e. Φ is $N \times K$). However, the complexity of the signal is reduced in a supervised manner to reflect exactly η effective degrees of freedom. Eq. 6.1 has an intuitive appeal compared to Eq. 3.13, both as a fully supervised counterpart to a principal components regression, and in the ease with which the hyperparameter η can be interpreted as the effective dimensionality of the data.

6.2. Future work

A discussion of the high-dimensional case, when $K \gg N$ has been omitted thus far. There are at least three approaches to estimating HFR parameters in an extremely high-dimensional setting: (i) Level-pruning, (ii) branch-pruning and (iii) level-regularization. The most natural approach is to prune the $K - N - 1$ lowest levels. This approach is simple to implement and ensures that only a minimal amount of idiosyncratic information is lost, with all predictors remaining in the regression. The level-specific parameter matrix $\hat{\mathbf{B}}$ now contains only the $K - N - 1$ upper levels and the optimization algorithm is not affected.

Instead of pruning entire levels, branches of the hierarchy could be pruned to permit high-dimensional estimation. Removing the conditional effects between unrelated clusters (i.e. replacing the respective entries in the lower triangle of \mathbf{H} with zero), the dimensionality of the problem is reduced. An example is to estimate a sparsely connected graph, such as a minimum spanning tree, where the conditional effect of nodes with no common parent is removed.¹¹ Finally, $\hat{\mathbf{B}}$ could be estimated using a penalized regression such as a ridge or a Lasso, resulting in an adaptive version of the HFR. This approach retains the full hierarchy, but introduces a second hyperparameter, controlling the strength of shrinkage of level-specific parameters.

Several additional avenues for the further development and application of the HFR exist. A generalization of the level-specific regressions to include different classes of response variables, such as a binomial response with a logistical link function, is an important extension to facilitate applications of the HFR to classification problems. Furthermore, the construction of \mathbf{S} has been kept deliberately simple, but could be expanded to accommodate non-nested or overlapping cluster structures, more sophisticated factor estimation methods (for instance by replacing the sum over child nodes with the principal component weights of the child nodes), or by regularizing the

¹¹Single-linkage agglomerative nesting, for instance, is particularly well-suited to the estimation of minimum spanning trees (Gower & Ross, 1969).

information content using tree-pruning techniques based on the information gain of each level.

The characteristics of the HFR make it particularly well-suited to regression applications with an underlying hierarchical or grouped data generating process, such as high-dimensional factor modeling in econometric analysis (e.g. nowcasting with dynamic factor models) or in finance (e.g. multi-factor asset pricing). Applications similar to the gene selection problem discussed in [Zou & Hastie \(2005\)](#) may also prove particularly suitable to the HFR. Finally, the methodology is not necessarily limited to regression or classification problems. By replacing level-specific regressions, for instance, with level-specific quadratic programs, hierarchical factor-based shrinkage can be applied to the weights obtained from traditional optimization techniques for financial portfolio construction, increasing the robustness of asset allocations in the presence of return clustering.

7. Concluding remarks

Prediction tasks with high-dimensional multicollinear predictor sets pose a challenge for least squares based fitting procedures, and a large and productive literature exists advancing various regularized approaches to addressing the issue. The HFR is a novel contribution to this body of knowledge, leveraging insights gained in the domains of machine learning and graph theory to proffer a useful and — in some respects — superior solution.

The information contained in predictors is partitioned into multiple levels of common and idiosyncratic components within a hierarchical tree structure. The parameters are subsequently estimated in such a manner as to reflect each of the information components partially, with the extent to which information is processed depending on a penalty on overall model complexity. This information theoretical approach results in a loss function that closely resembles an information criterion, trading off goodness-of-fit against parsimony.

The departure from a traditional penalized regression approach allows the HFR to perform well across a broad spectrum of regression tasks. Given group shrinkage targets, clusters of noise predictors can be shrunken to zero in a manner that does not require the remaining model parameters to shrink. This allows the HFR to produce good results in cases where estimators such as the ridge regression and PCR do not. Similarly, the factor structure permits the HFR to capture latent structures much like the PCR and PLSR. Finally, the estimator is particularly well-suited to grouped variable structures, which is generally solved only moderately well by traditional methods.

A series of simulations, as well as an empirical application are used in this paper to illustrate the performance of the HFR across these different settings and regression tasks. The application to a data set of economic growth determinants highlights an additional feature: the ability of the HFR to shed light on the level at which information enters the estimation process — i.e. the hierarchical level at which response variation is most adequately explained. By examining the contributions of individual variable clusters to the estimates, evidence is found for the existence of few broad regional or geographic factors that explain growth disparities, suggesting that the question of discovering individual growth determinants is perhaps misplaced, or needs to be performed conditional on regional peculiarities.

References

Alipour, E., Adolpsh, C., Zaribafyan, A. & Rounds, M. 2016. *Quantum-Inspired Hierarchical Risk Parity*. (White Paper). 1QBit.

Bach, F., Jenatton, R., Mairal, J. & Obozinski, G. 2012. Structured Sparsity through Convex Optimization. *Statistical Science*. 27(4):450–468.

Bair, E., Hastie, T., Paul, D. & Tibshirani, R. 2006. Prediction by Supervised Principal Components. *Journal of the American Statistical Association*. 101(473):119–137.

Bondell, H.D. & Reich, B.J. 2008. Simultaneous Regression Shrinkage, Variable Selection and Clustering of Predictors with OSCAR. *Biometrics*. 64(1):115–123.

Di Matteo, T., Aste, T. & Mantegna, R.N. 2004. An Interest Rates Cluster Analysis. *Physica A: Statistical Mechanics and its Applications*. 339(1-2):181–188.

Diebold, F.X. & Yilmaz, K. 2015. Measuring the Dynamics of Global Business Cycle Connectedness. in *Unobserved Components and Time Series Econometrics* Illustrated ed. S.J. Koopman & N. Shephard (eds.). Oxford University Press S.J. Koopman & N. Shephard (eds.). 45–70.

Efron, B., Hastie, T., Johnstone, I. & Tibshirani, R. 2004. Least Angle Regression. *Annals of Statistics*. 32(2):407–499.

Eicher, T.S., Papageorgiou, C. & Raftery, A.E. 2011. Default Priors and Predictive Performance in Bayesian Model Averaging, with Application to Growth Determinants. *Journal of Applied Econometrics*. 26(1):30–55.

Epshtain, B. & Ullman, S. 2005. Feature Hierarchies for Object Classification. in *Tenth IEEE International Conference on Computer Vision (ICCV'05) Volume 1* Beijing, China: IEEE. 220–227 Vol. 1.

Everitt, B., Landau, S., Stahl, D. & Leese, M. 2011. *Cluster analysis*. 5th ed ed. (Wiley series in probability and statistics). Chichester, West Sussex, U.K: Wiley.

Friedman, J., Hastie, T. & Tibshirani, R. 2001. *The Elements of Statistical Learning*. First ed. Vol. 1. Springer series in statistics Springer, Berlin.

Friedman, J., Hastie, T. & Tibshirani, R. 2010. Regularization Paths for Generalized Linear Models via Coordinate Descent. *Journal of Statistical Software*. 33(1).

Girshick, R., Donahue, J., Darrell, T. & Malik, J. 2014. Rich Feature Hierarchies for Accurate Object Detection and Semantic Segmentation. in *2014 IEEE Conference on Computer Vision and Pattern Recognition* Columbus, OH, USA: IEEE. 580–587.

Gower, J.C. & Ross, G.J.S. 1969. Minimum Spanning Trees and Single Linkage Cluster Analysis. *Applied Statistics*. 18(1):54–64.

Hansen, B.E. 2007. Least Squares Model Averaging. *Econometrica*. 75(4):1175–1189.

Hansen, B.E. 2019. *Econometrics*. Draft ed. University of Wisconsin.

Hoerl, A.E. 1962. Application of Ridge Analysis to Regression Problems. *Chemical Engineering Progress*. 58(3):54–59.

Hoerl, A.E. & Kennard, R.W. 1970. Ridge Regression: Biased Estimation for Nonorthogonal Problems. *Technometrics*. 12(1):55–67.

Hofmarcher, P., Cuaresma, J.C., Grun, B. & Hornik, K. 2011. *Fishing Economic Growth Determinants Using Bayesian Elastic Nets*. (Research Report Series 113). Wirtschaftsuniversität WIen: Institute for Statistics and Mathematics.

James, W. & Stein, C. 1961. Estimation with Quadratic Loss. *Proceedings of the Fourth Berkeley Symposium on Mathematical Statistics and Probability*. 1:361–380.

Jolliffe, I.T. 2002. *Principal Component Analysis*. Second ed. (Springer series in statistics). New York: Springer.

Kaufman, L. & Rousseeuw, P.J. 2005. *Finding Groups in Data: An Introduction to Cluster Analysis*. First ed. (Wiley series in probability and mathematical statistics). Hoboken, N.J: Wiley.

Kose, M.A., Otrok, C. & Whiteman, C.H. 2003. International Business Cycles: World, Region, and Country-Specific Factors. *The American Economic Review*. 93(4).

León, D., Aragón, A., Sandoval, J., Hernández, G., Arévalo, A. & Niño, J. 2017. Clustering Algorithms for Risk-Adjusted Portfolio Construction. *Procedia Computer Science*. 108(C):1334–

1343.

Ley, E. 2008. *On the Effect of Prior Assumptions in Bayesian Model Averaging with Applications to Growth Regression*. (MPRA Papers 6773).

Lopez de Prado, M. 2016. Building Diversified Portfolios that Outperform Out-of-Sample. *SSRN Electronic Journal*.

Maechler, M., Rousseeuw, P., Struyf, A. & Hornik, K. 2019. *Cluster: Cluster Analysis Basics and Extensions*. (R Package Version 2.1.0).

Maimon, O. & Rokach, L. 2010. *Data Mining and Knowledge Discovery Handbook*. Second ed. Boston, MA: Springer US.

Mallows, C.L. 1973. Some Comments on CP. *Technometrics*. 15(4):661–675.

Mantegna, R.N. 1999. Hierarchical Structure in Financial Markets. *The European Physical Journal B-Condensed Matter and Complex Systems*. 11(1):193–197.

Martens, H. 2001. Reliable and Relevant Modelling of Real World Data: A Personal Account of the Development of PLS Regression. *Chemometrics and Intelligent Laboratory Systems*. 58(2):85–95.

Mevik, B.-H. & Wehrens, R. 2019. Introduction to the pls Package. *R package manuals*.

Mishra, C. & Gupta, D.L. 2017. Deep Machine Learning and Neural Networks: An Overview. *IAES International Journal of Artificial Intelligence (IJ-AI)*. 6(2).

Pfitzinger, J. & Katzke, N. 2019. *A Constrained Hierarchical Risk Parity Algorithm with Cluster-Based Capital Allocation*. (Working Paper 14/2019). Stellenbosch University, Department of Economics.

R Core Team. 2018. *R: A Language and Environment for Statistical Computing*. Vienna, Austria: R Foundation for Statistical Computing.

Raffinot, T. 2016. Hierarchical Clustering based Asset Allocation. *SSRN Electronic Journal*.

Rey, H. 2015. Dilemma not Trilemma: The Global Financial Cycle and Monetary Policy Independence. *NBER Working Papers*. No. 21162.

Sala-I-Martin, X., Doppelhofer, G. & Miller, R.I. 2004. Determinants of Long-Term Growth: A Bayesian Averaging of Classical Estimates (BACE) Approach. *The American Economic Review*. 94(4).

Schneider, U. & Wagner, M. 2012. Catching Growth Determinants with the Adaptive Lasso: Lassoing Growth Determinants. *German Economic Review*. 13(1):71–85.

Simon, H.A. 1962. The Architecture of Complexity. *Proceedings of the American Philosophical Society*. 106(6):467–482.

Stock & Watson. 2016a. Dynamic Factor Models, Factor-Augmented Vector Autoregressions, and Structural Vector Autoregressions in Macroeconomics. in *Handbook of Macroeconomics* Vol. 2. Elsevier. 415–525.

Stock & Watson. 2016b. Factor Models and Structural Vector Autoregressions in Macroeconomics. *Handbook of Macroeconomics*. 2.

Tibshirani, R. 1996. Regression Shrinkage and Selection Via the Lasso. *Journal of the Royal Statistical Society: Series B (Methodological)*. 58(1):267–288.

Tibshirani, R., Saunders, M., Rosset, S., Zhu, J. & Knight, K. 2005. Sparsity and Smoothness via the Fused Lasso. *Journal of the Royal Statistical Society: Series B (Statistical Methodology)*. 67(1):91–108.

Tola, V., Lillo, F., Gallegati, M. & Mantegna, R.N. 2008. Cluster Analysis for Portfolio Optimization. *Journal of Economic Dynamics and Control*. 32(1):235–258.

Tumminello, M., Lillo, F. & Mantegna, R.N. 2010. Correlation, Hierarchies, and Networks in Financial Markets. *Journal of Economic Behavior & Organization*. 75(1):40–58.

Turlach, B.A., Venables, W.N. & Wright, S.J. 2005. Simultaneous Variable Selection. *Technometrics*. 47(3):349–363.

van Wieringen, W.N. 2020. *Lecture Notes on Ridge Regression*. (Paper 1509.09169). arXiv.org.

Varian, H.R. 2014. Big Data: New Tricks for Econometrics. *Journal of Economic Perspectives*. 28(2):3–28.

Wold, S. 2001. Personal Memories of the Early PLS Development. *Chemometrics and Intelligent*

Laboratory Systems. 58(2):83–84.

Yuan, M. & Lin, Y. 2006. Model Selection and Estimation in Regression with Grouped Variables. *Journal of the Royal Statistical Society: Series B (Statistical Methodology)*. 68(1):49–67.

Zeng, X. & Figueiredo, M.A.T. 2013. *A Novel Sparsity and Clustering Regularization*. (Paper 1310.4945). arXiv.org.

Zou, H. 2006. The Adaptive Lasso and Its Oracle Properties. *Journal of the American Statistical Association*. 101(476):1418–1429.

Zou, H. & Hastie, T. 2005. Regularization and Variable Selection via the Elastic Net. *Journal of the Royal Statistical Society: Series B (Statistical Methodology)*. 67(2):301–320.

Zou, H. & Zhang, H.H. 2009. On the Adaptive Elastic-Net with a Diverging Number of Parameters. *The Annals of Statistics*. 37(4):1733–1751.

Appendix A. Proof of Proposition 1

Proposition 1 can be shown to hold by demonstrating the equivalency to ordinary least squares coefficients. The proposition defines

$$\hat{\beta} = \mathbf{S}' \mathbf{Q}_{zz}^{-1} \mathbf{Q}_{zy}. \quad (\text{A.1})$$

Expanding the regression equation and calculating the inverse product results in

$$\hat{\beta} = \begin{bmatrix} \mathbf{S}_1 \\ \mathbf{S}_2 \\ \mathbf{S}_3 \end{bmatrix}' \begin{bmatrix} \mathbf{Q}_{11} & \mathbf{0} & \mathbf{0} \\ \mathbf{Q}_{21} & \mathbf{Q}_{22} & \mathbf{0} \\ \mathbf{Q}_{31} & \mathbf{Q}_{32} & \mathbf{Q}_{33} \end{bmatrix}^{-1} \begin{bmatrix} \mathbf{Q}_{1y} \\ \mathbf{Q}_{2y} \\ \mathbf{Q}_{3y} \end{bmatrix} \quad (\text{A.2})$$

$$= \begin{bmatrix} \mathbf{S}_1 \\ \mathbf{S}_2 \\ \mathbf{S}_3 \end{bmatrix}' \begin{bmatrix} \mathbf{Q}_{11}^{-1} & \mathbf{0} & \mathbf{0} \\ -\mathbf{Q}_{22}^{-1} \mathbf{Q}_{21} \mathbf{Q}_{11}^{-1} & \mathbf{Q}_{22}^{-1} & \mathbf{0} \\ \mathbf{Q}_{33}^{-1} \mathbf{Q}_{32} \mathbf{Q}_{22}^{-1} \mathbf{Q}_{21} \mathbf{Q}_{11}^{-1} - \mathbf{Q}_{33}^{-1} \mathbf{Q}_{31} \mathbf{Q}_{11}^{-1} & -\mathbf{Q}_{33}^{-1} \mathbf{Q}_{32} \mathbf{Q}_{22}^{-1} & \mathbf{Q}_{33}^{-1} \end{bmatrix} \begin{bmatrix} \mathbf{Q}_{1y} \\ \mathbf{Q}_{2y} \\ \mathbf{Q}_{3y} \end{bmatrix} \quad (\text{A.3})$$

$$= \begin{bmatrix} \mathbf{S}_1 \\ \mathbf{S}_2 \\ \mathbf{S}_3 \end{bmatrix}' \begin{bmatrix} \mathbf{Q}_{11}^{-1} \mathbf{Q}_{1y} \\ \mathbf{Q}_{22}^{-1} \mathbf{Q}_{2y} - \mathbf{Q}_{22}^{-1} \mathbf{Q}_{21} \mathbf{Q}_{11}^{-1} \mathbf{Q}_{1y} \\ \mathbf{Q}_{33}^{-1} \mathbf{Q}_{3y} - \mathbf{Q}_{33}^{-1} \mathbf{Q}_{32} \mathbf{Q}_{22}^{-1} \mathbf{Q}_{2y} - \mathbf{Q}_{33}^{-1} \mathbf{Q}_{31} \mathbf{Q}_{11}^{-1} \mathbf{Q}_{1y} + \mathbf{Q}_{33}^{-1} \mathbf{Q}_{32} \mathbf{Q}_{22}^{-1} \mathbf{Q}_{21} \mathbf{Q}_{11}^{-1} \mathbf{Q}_{1y} \end{bmatrix}. \quad (\text{A.4})$$

Here $\mathbf{Q}_{ij} = \mathbf{z}'_i \mathbf{z}_j$ and $\mathbf{Q}_{iy} = \mathbf{z}'_i y$. Using the definition of the projection matrix $\mathbf{P}_i = \mathbf{z}_i \mathbf{Q}_{ii}^{-1} \mathbf{z}'_i$, and substituting the definitions of \mathbf{Q}_{ij} and \mathbf{Q}_{iy} the above can be simplified to give

$$\hat{\beta} = \begin{bmatrix} \mathbf{S}_1 \\ \mathbf{S}_2 \\ \mathbf{S}_3 \end{bmatrix}' \begin{bmatrix} \mathbf{Q}_{11}^{-1} \mathbf{Q}_{1y} \\ \mathbf{Q}_{22}^{-1} \mathbf{z}_2 [\mathbf{I} - \mathbf{P}_1] y \\ \mathbf{Q}_{33}^{-1} \mathbf{z}_3 [\mathbf{I} - \mathbf{P}_2 - \mathbf{P}_1 + \mathbf{P}_2 \mathbf{P}_1] y \end{bmatrix} \quad (\text{A.5})$$

$$= \begin{bmatrix} \mathbf{S}_1 \\ \mathbf{S}_2 \\ \mathbf{S}_3 \end{bmatrix}' \begin{bmatrix} \mathbf{Q}_{11}^{-1} \mathbf{Q}_{1y} \\ \mathbf{Q}_{22}^{-1} \mathbf{z}_2 [\mathbf{I} - \mathbf{P}_1] y \\ \mathbf{Q}_{33}^{-1} \mathbf{z}_3 [\mathbf{I} - \mathbf{P}_2] [\mathbf{I} - \mathbf{P}_1] y \end{bmatrix}. \quad (\text{A.6})$$

Eq. A.6 stacks the level-specific estimates, where the preceding levels are partialled out of each

respective level-specific estimate. Note also that the nested nature of the hierarchical features implies that $[\mathbf{I} - \mathbf{P}_2][\mathbf{I} - \mathbf{P}_1]\mathbf{y} = [\mathbf{I} - \mathbf{P}_2]\mathbf{y}$, making the above exactly analogous to a stacked version of Eq. 3.2. Multiplying the matrix and using the simple trick that $\mathbf{S}'_i(\mathbf{z}'_i\mathbf{z}_i)^{-1}\mathbf{z}'_i\mathbf{z}_j = \mathbf{S}'_j \forall i > j$ allows Eq. A.6 to be simplified further, resulting in

$$\begin{aligned}\hat{\beta} = & \mathbf{S}'_1 \mathbf{Q}_{11}^{-1} \mathbf{Q}_{1y} + \mathbf{S}'_2 \mathbf{Q}_{22}^{-1} \mathbf{Q}_{2y} - \mathbf{S}'_1 \mathbf{Q}_{11}^{-1} \mathbf{Q}_{1y} + \mathbf{S}'_3 \mathbf{Q}_{33}^{-1} \mathbf{Q}_{3y} - \\ & \mathbf{S}'_2 \mathbf{Q}_{22}^{-1} \mathbf{Q}_{2y} - \mathbf{S}'_1 \mathbf{Q}_{11}^{-1} \mathbf{Q}_{1y} + \mathbf{S}'_1 \mathbf{Q}_{11}^{-1} \mathbf{Q}_{1y}.\end{aligned}\quad (\text{A.7})$$

Finally, recalling that $\mathbf{S}_3 = \mathbf{I}$, this simplifies to

$$\hat{\beta} = \mathbf{Q}_{33}^{-1} \mathbf{Q}_{3y}. \quad (\text{A.8})$$

Since $\mathbf{z}_3 = \mathbf{x}$, $\hat{\beta}$ is simply the ordinary least squares estimator:

$$\hat{\beta} = (\mathbf{x}' \mathbf{x})^{-1} \mathbf{x}' \mathbf{y} = \hat{\beta}_{\text{ols}}. \quad (\text{A.9})$$

Appendix B. Derivation of path-independent HFR estimates

Section 3.4 suggests that $\hat{\beta}_{\text{hfr}}$ can be reformulated to remove path-dependence from the level-specific estimates, with

$$\hat{\beta}_{\text{hfr}} = \hat{\mathcal{B}}\phi. \quad (\text{B.1})$$

To derive this result, recall once again the case with $K = 4$ and $L = 3$ presented in Section 3.2 and in [Appendix A](#). Here $\hat{\mathcal{B}} = [\hat{\mathbf{w}}_1 \dots \hat{\mathbf{w}}_L]$, with $\hat{\mathbf{w}}_\ell = \mathbf{S}'_\ell \mathbf{Q}_{\ell\ell}^{-1} \mathbf{Q}_{\ell y}$, using the notation in [Appendix A](#). In addition, ϕ is the transformation of the vector of shrinkage weights described in Section 3.4.

Eq. B.2 begins by restating Eq. A.2 with shrinkage weights:

$$\hat{\beta}_{\text{hfr}} = \begin{bmatrix} \mathbf{S}_1 \\ \mathbf{S}_2 \\ \mathbf{S}_3 \end{bmatrix}' \begin{bmatrix} \mathbf{Q}_{11} & \mathbf{0} & \mathbf{0} \\ \mathbf{Q}_{21} & \mathbf{Q}_{22} & \mathbf{0} \\ \mathbf{Q}_{31} & \mathbf{Q}_{32} & \mathbf{Q}_{33} \end{bmatrix} \odot \begin{bmatrix} \Theta_1 & \Theta_2 & \Theta_3 \end{bmatrix}^{-1} \begin{bmatrix} \mathbf{Q}_{1y} \\ \mathbf{Q}_{2y} \\ \mathbf{Q}_{3y} \end{bmatrix} \quad (\text{B.2})$$

$$= \begin{bmatrix} \mathbf{S}_1 \\ \mathbf{S}_2 \\ \mathbf{S}_3 \end{bmatrix}' \begin{bmatrix} \theta_1^{-1} \mathbf{Q}_{11} & \mathbf{0} & \mathbf{0} \\ \theta_1^{-1} \mathbf{Q}_{21} & \theta_2^{-1} \mathbf{Q}_{22} & \mathbf{0} \\ \theta_1^{-1} \mathbf{Q}_{31} & \theta_2^{-1} \mathbf{Q}_{32} & \theta_3^{-1} \mathbf{Q}_{33} \end{bmatrix}^{-1} \begin{bmatrix} \mathbf{Q}_{1y} \\ \mathbf{Q}_{2y} \\ \mathbf{Q}_{3y} \end{bmatrix}. \quad (\text{B.3})$$

Calculating the inverse and multiplying out in a manner analogous to Eqs. A.3 & A.4 in [Appendix A](#) reduces the above to

$$\begin{aligned} \hat{\beta}_{\text{hfr}} = & \theta_1 \mathbf{S}'_1 \mathbf{Q}_{11}^{-1} \mathbf{Q}_{1y} + \theta_2 \mathbf{S}_2 \mathbf{Q}_{22}^{-1} \mathbf{Q}_{2y} - \theta_2 \mathbf{S}_1 \mathbf{Q}_{11}^{-1} \mathbf{Q}_{1y} + \theta_3 \mathbf{S}_3 \mathbf{Q}_{33}^{-1} \mathbf{Q}_{3y} - \\ & \theta_3 \mathbf{S}_2 \mathbf{Q}_{22}^{-1} \mathbf{Q}_{2y} - \theta_3 \mathbf{S}'_1 \mathbf{Q}_{11}^{-1} \mathbf{Q}_{1y} + \theta_3 \mathbf{S}'_1 \mathbf{Q}_{11}^{-1} \mathbf{Q}_{1y}. \end{aligned} \quad (\text{B.4})$$

Using the definition of $\hat{\mathbf{w}}_\ell$ yields

$$\hat{\beta}_{\text{hfr}} = \hat{\mathbf{w}}_1(\theta_1 - \theta_2) + \hat{\mathbf{w}}_2(\theta_2 - \theta_3) + \hat{\mathbf{w}}_3(\theta_3) \quad (\text{B.5})$$

$$= \hat{\mathcal{B}}\phi, \quad (\text{B.6})$$

where

$$\phi = \begin{cases} \theta_\ell - \theta_{\ell+1} & \text{when } \ell < 3 \\ \theta_\ell & \text{otherwise.} \end{cases}$$

With the addition of an arbitrary number of levels, this result generalizes to the definition presented in Section 3.4.

Appendix C. Proof of Proposition 2

Proposition 2 asserts that the estimates obtained by solving the quadratic program in Eq. 3.13 are identical to the estimates obtained by minimizing Eq. 3.11, such that $\hat{\beta}_{\text{hfr};\theta_\lambda^*} = \hat{\beta}_{\text{qp};\phi_\lambda^*}$. Since the inequality constraints are identical in both equations, the derivation below abstracts from constraints.

Eq. C.1 restates the loss function of the HFR estimator introduced in Eq. 3.11, but substituting the definition of $\hat{\beta}_{\text{hfr}}$ from Eq. 3.12:

$$\mathcal{L}(\mathbf{x}, y) = N^{-1}(\mathbf{x}\hat{\mathbf{B}}\phi - y)'(\mathbf{x}\hat{\mathbf{B}}\phi - y) + \lambda\nu_{\text{eff}}. \quad (\text{C.1})$$

Setting $\partial\mathcal{L}/\partial\phi = \mathbf{0}$ to solve the optimization problem yields

$$\frac{\partial\mathcal{L}}{\partial\phi} = \mathbf{0} : N^{-1} \left(2\hat{\mathbf{B}}' \mathbf{x}' \mathbf{x} \hat{\mathbf{B}} \phi_\lambda^* - 2\hat{\mathbf{B}}' \mathbf{x}' y \right) + \lambda\nu = \mathbf{0}. \quad (\text{C.2})$$

Note that $\partial\nu_{\text{eff}}/\partial\phi = \nu$ in Eq. C.2. Multiplying out, rearranging and recalling that $\mathbf{x}\hat{\mathbf{B}} = \hat{\mathbf{y}}$ results in

$$\hat{\mathbf{B}}' \mathbf{x}' \mathbf{x} \hat{\mathbf{B}} \phi_\lambda^* = \hat{\mathbf{B}}' \mathbf{x}' y - \frac{N\lambda}{2} \nu \quad (\text{C.3})$$

$$\phi_\lambda^* = (\hat{\mathbf{y}}' \hat{\mathbf{y}})^{-1} \hat{\mathbf{y}}' y - \frac{N\lambda}{2} (\hat{\mathbf{y}}' \hat{\mathbf{y}})^{-1} \nu. \quad (\text{C.4})$$

In order to demonstrate that the solution ϕ_λ^* is equivalent to the quadratic program in 3.13, the calculation is repeated analogously for the case of $\hat{\beta}_{\text{qp}}$. The loss function is stated as

$$\mathcal{L}_{\text{qp}}(\mathbf{x}, y) = \frac{1}{2} \phi' \hat{\mathbf{y}}' \hat{\mathbf{y}} \phi - (\hat{\mathbf{y}}' y)' \phi + \frac{N\lambda}{2} \nu' \phi. \quad (\text{C.5})$$

Letting $\partial\mathcal{L}_{\text{qp}}/\partial\phi = \mathbf{0}$ results in

$$\frac{\partial \mathcal{L}_{\text{qp}}}{\partial \phi} = \mathbf{0} : \hat{\mathbf{y}}' \hat{\mathbf{y}} \phi_{\lambda}^* - \hat{\mathbf{y}}' \mathbf{y} + \frac{N\lambda}{2} \boldsymbol{\nu} = \mathbf{0} \quad (\text{C.6})$$

$$\phi_{\lambda}^* = (\hat{\mathbf{y}}' \hat{\mathbf{y}})^{-1} \hat{\mathbf{y}}' \mathbf{y} - \frac{N\lambda}{2} (\hat{\mathbf{y}}' \hat{\mathbf{y}})^{-1} \boldsymbol{\nu}. \quad (\text{C.7})$$

Eq. C.7 is identical to Eq. C.4, demonstrating that minimizing the quadratic program in Eq. 3.13 results in the solution that minimizes Eq. 3.11, and the respective parameter estimates $\hat{\boldsymbol{\beta}}_{\text{hfr};\theta_{\lambda}^*}$ and $\hat{\boldsymbol{\beta}}_{\text{qp};\phi_{\lambda}^*}$ are equivalent.

Given the definition of $\hat{\boldsymbol{\beta}}_{\text{hfr};\theta_{\lambda}^*} = \hat{\mathbf{B}} \phi_{\lambda}^*$ from Eq. 3.12, it follows that

$$\hat{\boldsymbol{\beta}}_{\text{hfr};\theta_{\lambda}^*} = \hat{\mathbf{B}} (\hat{\mathbf{y}}' \hat{\mathbf{y}})^{-1} \hat{\mathbf{y}}' \mathbf{y} - \frac{N\lambda}{2} \hat{\mathbf{B}} (\hat{\mathbf{y}}' \hat{\mathbf{y}})^{-1} \boldsymbol{\nu}. \quad (\text{C.8})$$

The first term does not depend on $\boldsymbol{\theta}$ and is simply equal to the vector of OLS estimates, such that

$$\hat{\boldsymbol{\beta}}_{\text{hfr};\theta_{\lambda}^*} = \hat{\boldsymbol{\beta}}_{\text{ols}} - \frac{N\lambda}{2} \hat{\mathbf{B}} (\hat{\mathbf{y}}' \hat{\mathbf{y}})^{-1} \boldsymbol{\nu}. \quad (\text{C.9})$$

Thus the optimal HFR estimates consist of OLS estimates and an adjustment term, $\frac{N\lambda}{2} \hat{\mathbf{B}} (\hat{\mathbf{y}}' \hat{\mathbf{y}})^{-1} \boldsymbol{\nu}$ that encapsulates the group mean shrinkage of the parameters, with the strength of shrinkage governed by λ . The ability to break the optimization down into separate components vastly reduces computation time for cross-validation procedures, since sub-components only need to be computed once.